

NAVAL POSTGRADUATE SCHOOL

Monterey, California



THESIS

**A ROBUST METHODOLOGY TO EVALUATE
AIRCRAFT SURVIVABILITY ENHANCEMENT
DUE TO COMBINED SIGNATURE REDUCTION
AND ONBOARD ELECTRONIC ATTACK**

by

Brian M. Flachsbart

June, 1997

Thesis Advisor:
Second Reader:

Robert E. Ball
James R. Powell

Approved for public release; distribution is unlimited.

[DTIC QUALITY INSPECTED 3]

19970925 047

REPORT DOCUMENTATION PAGE

Form Approved
OMB No. 0704-0188

Public reporting burden for this collection of information is estimated to average 1 hour per response, including the time for reviewing instruction, searching data sources, gathering and maintaining the data needed, and completing and reviewing the collection of information. Send comments regarding this burden estimate or any other aspect of this collection of information, including suggestions for reducing this burden, to Washington headquarters Services, Directorate for Information Operations and Reports, 1215 Jefferson Davis Highway, Suite 1204, Arlington, VA 22202-4302, and to the Office of Management and Budget, Paperwork Reduction Project (0704-0188) Washington DC 20503.

1. AGENCY USE ONLY <i>(Leave blank)</i>	2. REPORT DATE June 1997	3. REPORT TYPE AND DATES COVERED Master's Thesis
4. TITLE AND SUBTITLE A ROBUST METHODOLOGY TO EVALUATE AIRCRAFT SURVIVABILITY ENHANCEMENT DUE TO COMBINED SIGNATURE REDUCTION AND ONBOARD ELECTRONIC ATTACK		5. FUNDING NUMBERS
6. AUTHOR(S) Flachsbart, Brian M.		8. PERFORMING ORGANIZATION REPORT NUMBER
7. PERFORMING ORGANIZATION NAME(S) AND ADDRESS(ES) Naval Postgraduate School Monterey, CA 93943-5000		
9. SPONSORING / MONITORING AGENCY NAME(S) AND ADDRESS(ES)		10. SPONSORING / MONITORING AGENCY REPORT NUMBER
11. SUPPLEMENTARY NOTES The views expressed in this thesis are those of the author and do not reflect the official policy or position of the Department of Defense or the U.S. Government.		
12a. DISTRIBUTION / AVAILABILITY STATEMENT Approved for public release; distribution unlimited.		12b. DISTRIBUTION CODE
13. ABSTRACT <i>(maximum 200 words)</i> This thesis examines the effect of combining radar signature reduction and onboard electronic attack (EA) capability on the survivability enhancement of a generic joint strike fighter (JSF). The missions of a generic JSF are examined, and a tactical scenario for an air-to-air mission and a strike mission are presented. The principles of signature reduction and EA using onboard Electronic Countermeasures (ECM) are reviewed. The effect of signature level and of jammer effective radiated power (JERP) on the ability of a radar to detect the JSF are determined individually. Finally, an approach for combining the two survivability enhancement features is described, in the context of the two tactical JSF scenarios, and an EXCEL spreadsheet program entitled RCS-JERP is developed using unclassified radar and EA equipment data. Although all of the material in this thesis and in RCS-JERP are unclassified, the principles, methodology, and spreadsheet can be applied to specific (and classified) scenarios by utilizing the specific radar data, applicable mission threat analyses, and the effectiveness of the specific EA techniques employed.		
14. SUBJECT TERMS Aircraft Combat Survivability; Susceptibility; Radar Cross Section; Signature Reduction; Electronic Attack; Noise Jamming and Deceiving; Signal-to-Noise Ratio; Jam-to-Signal Ratio; Signal-to-Interference Ratio; Joint Strike Fighter;		15. NUMBER OF PAGES 71
17. SECURITY CLASSIFICATION OF REPORT Unclassified		16. PRICE CODE
18. SECURITY CLASSIFICATION OF THIS PAGE Unclassified	19. SECURITY CLASSIFICATION OF ABSTRACT Unclassified	20. LIMITATION OF ABSTRACT UL

NSN 7540-01-280-5500

Standard Form 298 (Rev. 2-89)
Prescribed by existing ANSI Std. Z39-18

Approved for public release; distribution is unlimited

A ROBUST METHODOLOGY TO EVALUATE AIRCRAFT SURVIVABILITY
ENHANCEMENT DUE TO COMBINED SIGNATURE REDUCTION
AND ONBOARD ELECTRONIC ATTACK

Brian M. Flachsbart
Lieutenant Commander, United States Navy
B.S., United States Naval Academy, 1986

Submitted in partial fulfillment of the
requirements for the degree of

MASTER OF SCIENCE IN AERONAUTICAL ENGINEERING

from the

NAVAL POSTGRADUATE SCHOOL
June 1997

Author:

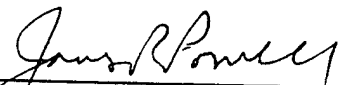


Brian M. Flachsbart

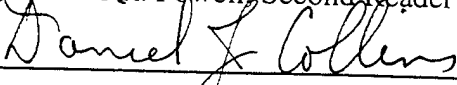
Approved by:



Robert E. Ball, Thesis Advisor



James R. Powell, Second Reader



Daniel J. Collins, Chairman
Department of Aeronautics & Astronautics

ABSTRACT

This thesis examines the effect of combining radar signature reduction and onboard electronic attack (EA) capability on the survivability enhancement of a generic joint strike fighter (JSF). The missions of a generic JSF are examined, and a tactical scenario for an air-to-air mission and a strike mission are presented. The principles of signature reduction and EA using onboard Electronic Countermeasures (ECM) are reviewed. The effect of signature level and of jammer effective radiated power (JERP) on the ability of a radar to detect the JSF are determined individually. Finally, an approach for combining the two survivability enhancement features is described, in the context of the two tactical JSF scenarios, and an EXCEL spreadsheet program entitled RCS-JERP is developed using unclassified radar and EA equipment data. Although all of the material in this thesis and in RCS-JERP are unclassified, the principles, methodology, and spreadsheet can be applied to specific (and classified) scenarios by utilizing the specific radar data, applicable mission threat analyses, and the effectiveness of the specific EA techniques employed.

TABLE OF CONTENTS

I.	INTRODUCTION.....	1
	A. THE SURVIVABILITY PROBLEM.....	1
	B. DEFINITIONS.....	1
	1. Survivability	2
	2. Susceptibility	2
	3. Vulnerability	3
	C. THE EFFECT OF SIGNATURES AND ONBOARD ELECTRONIC ATTACK (EA) CAPABILITIES ON SUSCEPTIBILITY.....	3
	D. THE BOTTOM LINE--HOW SMALL SHOULD THE RCS BE, AND HOW MUCH ONBOARD EA EQUIPMENT POWER DO WE NEED?	4
II.	THE GENERIC JOINT STRIKE FIGHTER (JSF) AND ITS MISSIONS	7
	A. JSF DESCRIPTION.....	7
	B. JSF MISSIONS.....	7
	1. Combat Air Patrol (CAP)	7
	2. Fighter Escort (FE)	7
	3. Deck Launched Interceptor (DLI)	8
	4. Suppression of Enemy Air Defenses (SEAD)	8
	5. Interdiction.....	8
	6. War-at-Sea (WAS).....	9
	7. Close Air Support (CAS)	9
	C. MISSION THREAT ANALYSIS.....	9
	1. Air-to-Air Missions	9
	2. Strike Missions.....	11
	3. Jammer Employment	12
III.	SIGNATURE REDUCTION AND SUSCEPTIBILITY REDUCTION CONCEPTS AND EQUATIONS	15
	A. AIRCRAFT RADAR CROSS SECTION (RCS).....	15
	1. RCS Shape (Magnitude and Azimuth).....	15
	2. How RCS is Reduced	16
	B. RADAR DETECTION AND THE EFFECT OF SIGNATURE REDUCTION	17
	C. COUNTERING SIGNATURE REDUCTION	26
IV.	ONBOARD ELECTRONIC ATTACK AND SUSCEPTIBILITY REDUCTION	27
	A. NOISE JAMMING AND DECEIVING	27
	1. Noise Jamming.....	29

2. Range Gate Pull Off (RGPO).....	31
3. Velocity Gate Pull Off (VGPO)	32
4. Inverse Gain Scan.....	32
5. Cross Eye	33
6. Cross Polarization.....	34
B. JAMMING SUMMARY	35
V. SURVIVABILITY ENHANCEMENT DUE TO COMBINED SIGNATURE REDUCTION AND ELECTRONIC ATTACK.....	37
A. SIGNATURE REDUCTION AND ELECTRONIC ATTACK COMBINED.....	37
B. ADDITIONAL INFORMATION AND DATA PRESENTATION	44
1. Addition of Cost Data.....	44
2. Evaluating Different Deception Techniques.....	45
3. Different Data Presentations	45
VI. SUMMARY, CONCLUSIONS, AND RECOMMENDATIONS	47
APPENDIX.....	49
LIST OF REFERENCES.....	51
SELECTED BIBLIOGRAPHY.....	53
INITIAL DISTRIBUTION LIST.....	55

LIST OF FIGURES

FIGURE I-1: ENCOUNTER TREE DIAGRAM (AFTER BALL, 1997)	2
FIGURE II-1: BEYOND VISUAL RANGE (BVR) AIR-TO-AIR ENGAGEMENT - JSF TACTICALLY DISADVANTAGED..	10
FIGURE II-2: BVR AIR-TO-AIR ENGAGEMENT - JSF WITH TACTICAL ADVANTAGE	10
FIGURE II-3: TACTICALLY DISADVANTAGED JSF STRIKE AIRCRAFT.....	11
FIGURE II-4: JSF STRIKE AIRCRAFT WITH TACTICAL ADVANTAGE.....	12
FIGURE III-1: TYPICAL AIRCRAFT RCS (AFTER SKOLNIK)	16
FIGURE III-2: SIMPLIFIED RCS WITH FORWARD QUARTER REDUCTIONS.....	16
FIGURE III-3: RCS WITH ALL ASPECT REDUCTIONS.....	17
FIGURE III-4: TYPICAL RADAR TRANSMISSION PATH.....	19
FIGURE III-5: SIGNAL TO NOISE THRESHOLD.....	20
FIGURE III-6: NOISE ADDED VECTORIALLY	22
FIGURE III-7: RCS VS. RANGE FOR AIR-TO-AIR RADAR (S/N = 20).....	25
FIGURE III-8: RCS VS. RANGE FOR STRIKE RADAR (S/N = 10).....	25
FIGURE IV-1: SIGNAL + NOISE + JAMMING	29
FIGURE IV-2: CONSCAN RADAR RETURN FLUCTUATING DUE TO TARGET PRESENCE	32
FIGURE IV-3: CONSCAN RADAR RETURN PLUS INVERSE GAIN JAMMING	33
FIGURE IV-4: CROSS EYE REPEATER JAMMING IMPLEMENTATION	34
FIGURE V-1: RADAR PATH WITH JAMMING.....	37
FIGURE V-2: AIR-TO-AIR SCENARIO WITH NOISE JAMMING (RANGE = 35KM)	42
FIGURE V-3: AIR-TO-AIR SCENARIO WITH DECEPTION JAMMING (RANGE = 35KM)	42
FIGURE V-4: STRIKE SCENARIO WITH NOISE JAMMING (RANGE = 11KM).....	43
FIGURE V-5: STRIKE SCENARIO WITH DECEPTION JAMMING (RANGE = 11KM).....	43
FIGURE V-6: SIGNAL-TO-INTERFERENCE RATIO VERSUS RCS FOR SLOTBACK RADAR SCENARIO (RANGE = 35KM)	45
FIGURE V-7: RANGE VERSUS RCS FOR SLOTBACK RADAR SCENARIO WITH NOISE JAMMING (S/I = 0.25).....	46

LIST OF TABLES

TABLE III-1: TYPICAL RADAR PARAMETERS	24
TABLE IV-1: RADAR JAMMING TECHNIQUES (AFTER SCHLEHER, 1986).....	35
TABLE IV-2: REPRESENTATIVE ULQ-21 TECHNIQUES.....	36
TABLE V-1: TYPICAL RATIO VALUES.....	38
TABLE V-2: SUMMARY OF REPRESENTATIVE VALUES	41

ACKNOWLEDGMENT

The author thanks his thesis advisor, Dr. Robert Ball, for his encouragement, patient tutelage, and insightful probing. The expert guidance he provided made this an extremely enjoyable and broadening learning experience, in more than just the academic arena. The author also thanks Dr. Jeffrey Knorr for the many hours he spent thoroughly explaining the operation and design of radars and antennas, both in class and out. An additional debt of gratitude is due two fellow students, Jaime Engdahl for his ability to translate a one hour lecture into a 15 minute explanation even a pilot could understand, and Mike Overs for the numerous editing and sanity checks he performed.

The author gratefully acknowledges the financial support of COL Nolan Schmidt, USMC, PMA-272. Travel funding provided early in this process enabled attendance at an extremely informative and eye-opening radar and EW conference. Furthermore, the author thanks his father for essential editing advice and for putting up with him during his formative years, thus allowing him to survive long enough to write this. Finally, and most importantly, the author gratefully appreciates the love and support of his wife, Sylvia, during this two year endeavor.

I. INTRODUCTION

A. THE SURVIVABILITY PROBLEM

Maintaining combat effectiveness during sustained combat operations leaves little tolerance for operational losses, particularly for carrier-based operations. This mandates that modern aircraft be designed to survive in combat. Incorporation of survivability enhancement features results in the probability of survival (P_s) asymptotically approaching unity as more features are added. These survivability features and improvements, however, can be costly. Theoretically, an infinite pot of money could purchase total survivability. However, in order to achieve and maintain numerical superiority with a "reasonable number of acceptably survivable aircraft," a level of "optimum survivability" must be found. This optimal level will provide the most cost-effective mix of quantity (platforms fielded) and quality (incorporation of survivability enhancement features).

The probability of survival is the complement of the probability of kill, P_k . In simple probability terms, $P_s = 1 - P_k$. Many events must occur sequentially for an aircraft to be killed by a threat weapon system in a one-on-one encounter. Considering a guided missile threat, the system must be activated, it must detect the aircraft, it must track the aircraft, it must launch a missile, the missile must fly a proper intercept, and the missile must hit the aircraft or a proximity-fuzed high explosive warhead must be detonated. Finally, the damage caused by the hit or detonation must be sufficient to kill the aircraft. Each link in this chain of events must occur for the aircraft to be killed. An encounter tree diagram that represents this chain of events, is shown in Figure I-1, where each event or branch is represented by a probability. In summary,

$$P_{\text{kill}} = (P_{\text{Activated}})(P_{\text{Detect/Activated}})(P_{\text{Track/Detect}})(P_{\text{Launch/Track}})(P_{\text{Intercept/Launch}})(P_{\text{Hit/Intercept}})(P_{\text{Kill/Hit}}).$$

Degrading any of the right side branches (probabilities) in the tree results in the aircraft surviving the engagement with a higher probability.

B. DEFINITIONS

The Department of Defense published MIL-STD-2089 in July 1981 for the purpose of standardizing the definitions of survivability related terms. In accordance with that document, the following definitions are provided.

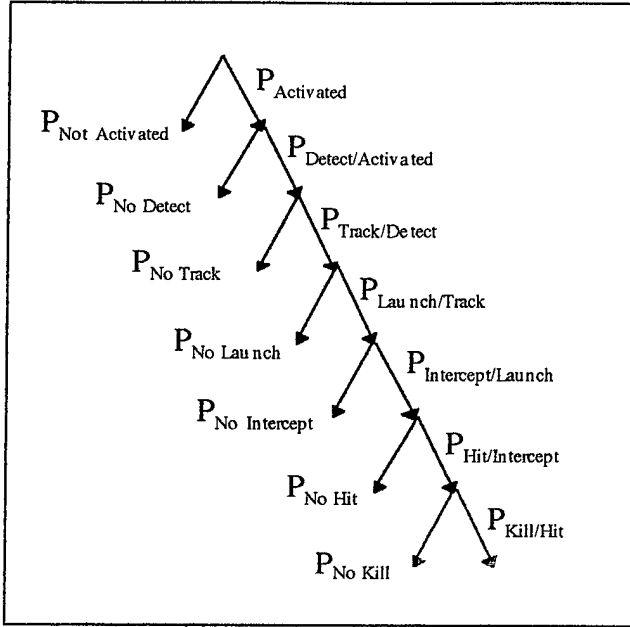


Figure I-1: Encounter Tree Diagram (after Ball, 1997)

1. Survivability

MIL-STD-2089 defines survivability as “the capability of an aircraft to avoid or withstand a man-made hostile environment without sustaining an impairment of its ability to accomplish its designated mission.” In terms of the tree diagram above, the goal of a survivability engineer is to degrade the probabilities associated with the right hand branches in the tree diagram. When evaluated from the perspective of aircrew anxiety, degrading early branches is better than degrading later branches--defeating missiles on the rail is always preferable to being hit but not killed.

2. Susceptibility

Susceptibility is defined as “the degree to which a device, equipment, or weapons system is open to effective attack due to one or more inherent weaknesses.” The susceptibility branch of the survivability discipline searches for ways to prevent the aircraft from being hit. Susceptibility reductions involve the incorporation of features or techniques that degrade early branches, up to and including the aircraft being hit. These features fall into six general categories: threat warning,

jamming and deceiving, signature reduction, expendables, threat suppression, and tactics (Ball, 1985).

3. Vulnerability

Vulnerability is defined as "the characteristics of a system which cause it to suffer a definite degradation (incapability to perform the designated mission) as a result of having been subjected to a certain level of effects in an unnatural (manmade) hostile environment." The vulnerability branch of the survivability discipline attempts to "harden" the aircraft to prevent a kill, given that the aircraft is hit. Vulnerability reduction techniques also fall into six general categories: component redundancy with separation, component location, passive damage suppression, active damage suppression, component shielding, and component elimination (Ball, 1985).

C. THE EFFECT OF SIGNATURES AND ONBOARD ELECTRONIC ATTACK (EA) CAPABILITIES ON SUSCEPTIBILITY

Susceptibility, as defined above, involves the first six branches in the encounter tree diagram. Of the six susceptibility reduction concepts, signature reduction stands alone as the one concept that is absolutely best when designed into the aircraft from the beginning. Threat warning systems, countermeasures systems, expendables systems, threat suppression, and tactics can all be developed and added after the aircraft is produced, although at some cost. Airframe modifications to reduce signatures, however, tend to be very expensive and only moderately effective when added later. Thus, the aircraft signature is a significant concern during the early design phase. Where does one look for guidance on how small the signature must be? If the signature requirement is set at a very small level, the aircraft runs the risk of being too expensive to purchase in large quantities. If the signature level is permitted to be too large, the aircraft risks experiencing unacceptable attrition levels, which would ultimately result in limiting the mission effectiveness of the aircraft.

When dealing with radar SAMs, the most important signature to reduce is the radar signature, or radar cross section (RCS) of the aircraft. (For the remainder of this thesis, "reduction of RCS" and "signature reduction" will be used interchangeably.) The aircraft RCS is a factor early in the encounter tree diagram. It primarily affects the threat system's ability to detect the aircraft as the aircraft flies on its mission. Reducing the RCS reduces the range at which the

aircraft can be detected, given that the threat is active. ("Given that the threat is active" acknowledges that early warning radars, which typically operate at lower frequencies and are less affected by RCS reductions, may have detected the aircraft and alerted the threat sites, making them active.)

Jamming and deceiving are susceptibility reduction concepts designed to prevent the threat radar from initially detecting the aircraft radar return or from being able to accurately track the aircraft once detection occurs. Once detected and tracked, the ability of the threat system to guide a missile to a successful intercept can be degraded by employing noise jamming and deceiving. Thus, if it is too expensive to reduce the RCS to levels that result in the desired survivability for the specified missions, the incorporation of onboard EA techniques and equipment, in conjunction with a moderate reduction in RCS, can provide a cost effective method of achieving the desired survivability.

D. THE BOTTOM LINE--HOW SMALL SHOULD THE RCS BE, AND HOW MUCH ONBOARD EA EQUIPMENT POWER DO WE NEED?

The answer to this question is driven by the mission-threat analysis. This analysis of how the aircraft is expected to be utilized, against an estimate of the projected threat, will form the basis of determining what sort of tactical advantage must be provided. Tactical advantage is the ability to get the first lethal shot off in any engagement. It is achieved by providing survivability enhancement features, e.g., low RCS level and powerful EA equipment (a jammer), such that the aircraft can close to a range that will allow the first lethal shot, without being killed. This thesis assumes that it is desirable to achieve as much of that tactical advantage as possible (affordable) with reduction in the aircraft RCS.

Any reduction in RCS results in a reduced detection range with corresponding reduction in the jammer power required to prevent detection or to deceive the threat. It also may allow the employment of better jamming techniques that may be more effective against the projected threat. These techniques may require greater jammer power for effectiveness. How much EA is needed will depend on how much of the required tactical advantage was not achieved through RCS reduction.

Associated with both RCS reduction and EA equipment power are costs. Of great interest is the combination of RCS level and EA power that results in minimum cost for a given level of

survivability. Since missions the aircraft must perform drive aircraft requirements, a set of typical missions must be selected. For the purpose of this report, missions of a generic Joint Strike Fighter (JSF) were chosen. To answer the question “what combination of RCS level and EA capabilities results in a minimum cost for a given level of survivability?,” this report develops a robust methodology that can be used to evaluate what combinations of RCS level and EA power provide the survivability required of the JSF in those mission areas. The costs of these combinations are to be determined in other studies.

II. THE GENERIC JOINT STRIKE FIGHTER (JSF) AND ITS MISSIONS

A. JSF DESCRIPTION

The generic joint strike fighter is a multi-role aircraft capable of performing both strike and fighter type missions. It is capable of filling the mission roles of the AV-8B Harrier, the A-10 Thunderbolt II, the F-14 Tomcat, the F-16 Falcon, and the F/A-18 Hornet. As such, it must provide air superiority as well as achieve self-escort strike capability. To be affordable, it must be an efficient compromise between fighter attributes and strike attributes. It must have adequate range capability to enable it to carry the fight to the enemy, it must have sufficient payload to inflict precise damage upon arrival, and it must be survivable.

B. JSF MISSIONS

The JSF can be expected to perform in the general mission areas of a strike fighter, which include both strike and air-to-air missions. These general strike fighter mission areas can be broken down into many specific missions. A brief, unclassified description of several specific missions are described below.

1. Combat Air Patrol (CAP)

The CAP mission consists of providing air superiority in a specific area. Its many variations include target area CAP (TARCAP), barrier CAP (BARCAP), and MIGCAP. These missions typically involve precise navigation to deconflict sectors, the penetration of enemy air defenses if required, as well as the influencing, countering, targeting, and destruction of airborne threats if necessary.

2. Fighter Escort (FE)

The Fighter Escort mission consists of providing air superiority for strike missions. The purpose of this mission is to prevent enemy fighters from interfering with a strike package during the transit to the target. It involves precise navigation to maintain position relative to the strike

package; the penetration of enemy air defenses; as well as the influencing, countering, targeting and destruction of airborne threats if required.

3. Deck Launched Interceptor (DLI)

The DLI mission consists of a rapid transition from a cold start to maximum energy addition in order to intercept enemy airborne threats as far away from base as possible. Typically scrambled from an alert posture, this mission involves long range detection, acquisition, targeting, and missile employment against threat aircraft and missiles.

4. Suppression of Enemy Air Defenses (SEAD)

The SEAD mission consists of negating enemy air defenses or the integrated air defense system (IADS). In its most common application, this means committing anti-radiation missiles (ARMs) against threat SAM systems. It involves precise navigation and timing to coordinate the attack, penetration of enemy air defenses if required, and the acquisition, tracking, and targeting of ground based emitters. The weapon of choice for SEAD missions is the High speed Anti-Radiation Missile (HARM). SEAD can range in scope from being the overall mission objective (e.g. sequential threat roll back) to being a support mission during a coordinated strike.

5. Interdiction

The Interdiction mission consists of attacking ground targets beyond the Forward Edge of the Battle Area (FEBA). The purpose of this type mission is to prevent the enemy from conducting operations in a specific area or to reduce the enemy's ability to wage war through the destruction of high value targets. It involves the penetration of enemy air defenses, precise navigation to avoid threat concentrations, countering of airborne threats if required, and the acquisition, targeting, and/or tracking of ground targets.

A variant of interdiction is the "surgical strike," a one-time mission with clearly defined goals achievable on a single attack. This type strike is not part of a sustained campaign, but is designed to capitalize on the element of surprise associated with a one-time event. As such, it must be prepared to confront the enemy IADS in its fully operational condition. Therefore, it does not

have the luxury of prolonged SEAD support to roll back the threat before committing a strike package.

6. War-at-Sea (WAS)

The WAS mission consists of attacking sea-based targets. The target in this case is highly mobile and collocated with numerous SAM threats. It involves tight coordination with other assets (particularly SEAD), penetration of enemy air defenses, and the acquisition, targeting, and tracking of enemy ships.

7. Close Air Support (CAS)

The CAS mission consists of attacking ground targets in support of friendly ground troops at, or near, the forward edge of the battle area (FEBA). The close proximity to friendly troops makes the CAS mission very demanding. It involves extremely precise navigation and timing to prevent inadvertently endangering friendly troops, the penetration of enemy air defenses, and the acquisition, targeting, and/or tracking of ground targets.

C. MISSION THREAT ANALYSIS

1. Air-to-Air Missions

Current aircraft that could be a threat to the JSF, such as the Mig-29 Fulcrum, possess significantly improved air-to-air missiles with increased range capabilities. The estimated range of the AA-10 Alamo is 50 - 110 km and the AIM-120 AMRAAM is 50 km (Jane's All the World's Aircraft, 1996). Thus, U.S. Forces currently lack a modern missile with an equivalent range and are at a distinct tactical disadvantage in terms of a long range missile capability. This results in threat aircraft possessing the capability to achieve first launch or simultaneous launch against U.S. aircraft at long ranges, as shown in Figure II-1.

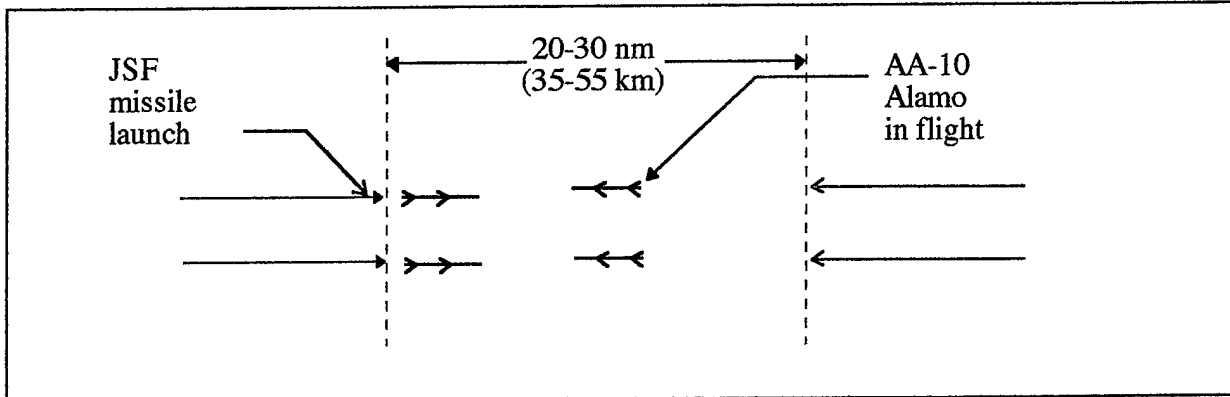


Figure II-1: Beyond Visual Range (BVR) Air-to-Air Engagement - JSF Tactically Disadvantaged

One way to regain the tactical advantage is to decrease the launch range of the AA-10 through the use of RCS reduction and EA capabilities. An acceptable tactical advantage in air-to-air missions would be realized if the JSF possessed RCS reduction and EA capabilities such that it could prosecute an intercept to arrive within 18-20 nm, or approximately 35 km, of the threat aircraft, while denying the threat aircraft the opportunity to “target” the JSF, where targeting is defined as detecting the JSF and generating and maintaining a track file suitable for weapons launch. This is depicted in Figure II-2.

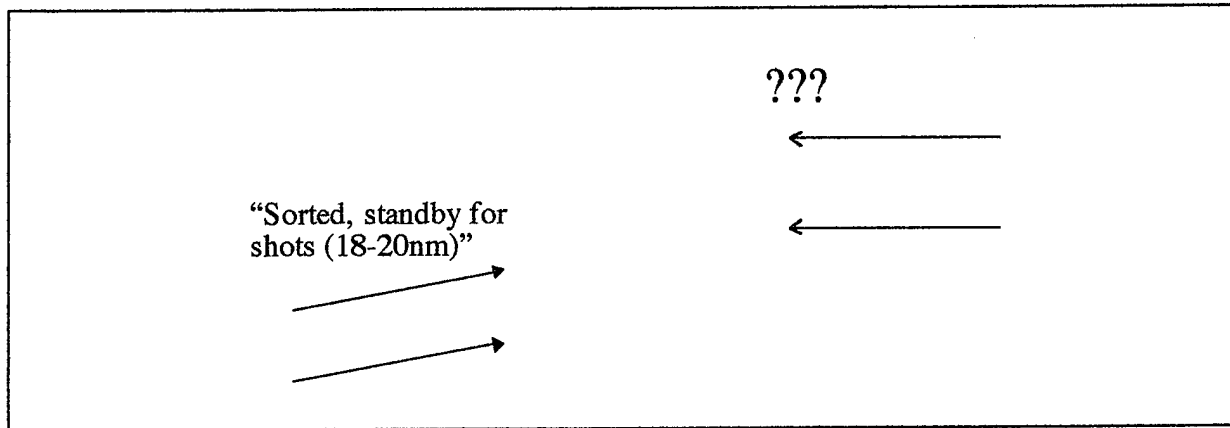


Figure II-2: BVR Air-to-Air Engagement - JSF With Tactical Advantage

This scenario assumes the JSF has the capability to utilize Low Probability of Intercept (LPI) radar modes for targeting and sorting, i.e., modes that will not trigger a radar warning receivers (RWR) on the threat aircraft. Another requirement is that the JSF can commit missiles from LPI track files or a Link-16 track file.

Thus, the goal for the air-to-air mission is to determine those combinations of RCS level and EA power that allow the JSF to close within 35 km of a representative threat aircraft without being targeted. This acknowledges that the JSF may be detected, but the threat aircraft is unable to generate and maintain a track file suitable for weapons launch. For the purpose of analysis, the Mig-29 Fulcrum with Slotback radar has been chosen as the representative threat aircraft.

2. Strike Missions

Current threat SAM systems have a significant range advantage over attacking aircraft employing conventional weapons. Furthermore, SAM systems are frequently collocated with high value targets, forcing the attacking aircraft to directly penetrate the enemy SAM rings. This leaves strike aircraft at a tactical disadvantage when attacking defended targets, as seen in Figure II-3.

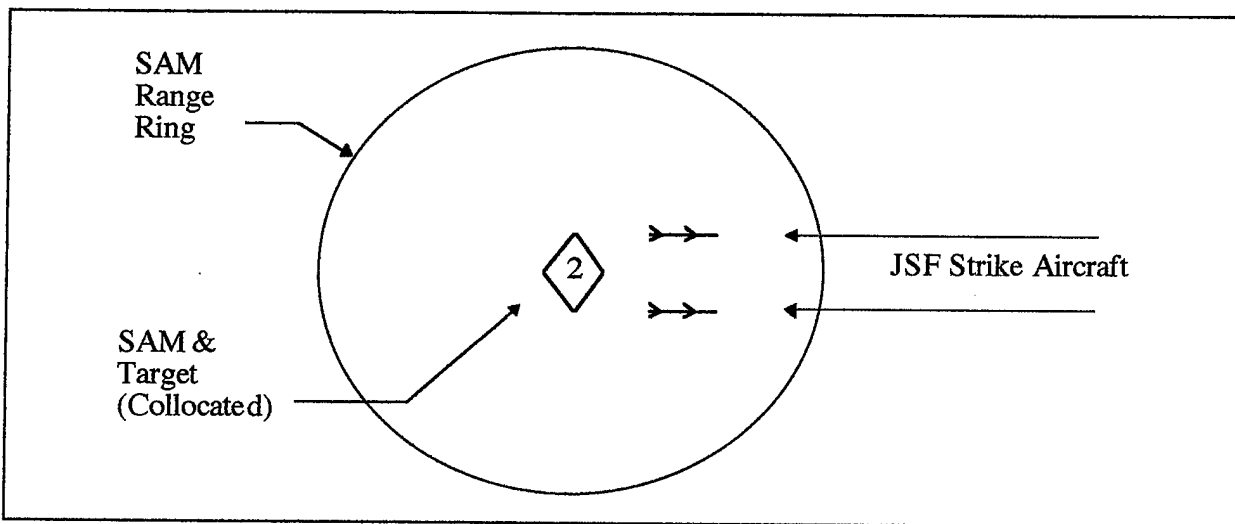


Figure II-3: Tactically Disadvantaged JSF Strike Aircraft

Current tactics and weapon acquisition programs attempt to reduce this disadvantage by emphasizing standoff. The Joint Stand Off Weapon (JSOW), the Joint Direct Attack Munition (JDAM), and the Standoff Land Attack Missile (SLAM) are examples of this approach, the least expensive being JDAM. In spite of this, current strike aircraft are still at a tactical disadvantage against most threat SAM systems. An acceptable tactical advantage on strike missions would be realized if the JSF could close to within JDAM range (assumed for the purposes of this report to be 6 nm, or approximately 11 km) of a SAM without being tracked accurately enough to be targeted by the SAM, as seen in Figure II-4.

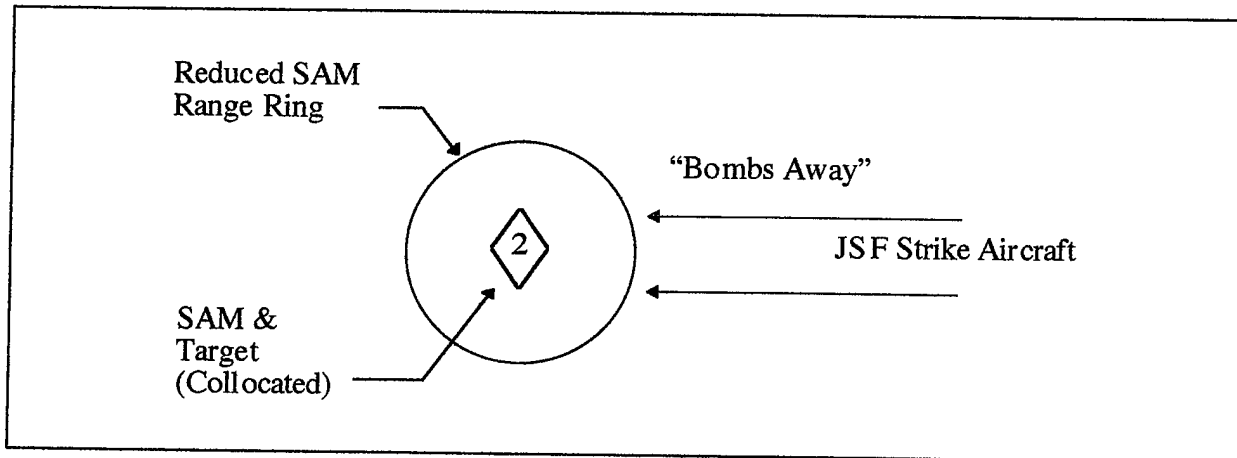


Figure II-4: JSF Strike Aircraft with Tactical Advantage

In addition, SEAD missions would benefit greatly from the ability to attack the enemy IADS from shorter range. SEAD aircraft would then be capable of achieving a “hard kill” on a SAM with an inexpensive JDAM rather than an expensive HARM. In addition, bomb damage assessment (BDA) would be much easier. Thus, the goal for strike and SEAD missions is to determine those combinations of RCS level and EA power that allow the JSF to close to within 11 km of a representative SAM site without being tracked accurately enough for the SAM to commit a missile. The SA-2E with the Fansong radar has been chosen as a representative SAM system for the purpose of this analysis due to the availability of unclassified data. The SA-6 would be a better choice as a more modern threat, however, required radar data does not exist at the unclassified level.

If the desired tactical advantage is unachievable using JDAM, an alternate mission threat analysis could be performed using the greater standoff capabilities (and greater cost) of JSOW. Ultimately, it is up to the warfighters to determine mission requirements with which to conduct mission threat analyses.

3. Jammer Employment

The onboard jammer is used to degrade detection, tracking and guidance. Employed incorrectly, EA can become a beacon, highlighting the aircraft when it would otherwise not have been detected. To be effective, it is vital that the jammer employ coherent, smart techniques, and not function as a beacon, which can be the case with noise jamming, and that tactics be developed

regarding when to radiate during operational scenarios. For the purpose of this report, it is assumed that appropriate tactics are developed governing the operational use of EA.

III. SIGNATURE REDUCTION AND SUSCEPTIBILITY REDUCTION CONCEPTS AND EQUATIONS

A. AIRCRAFT RADAR CROSS SECTION (RCS)

Radars “detect” objects actively by transmitting an electromagnetic wave in a pulse form and “listening” for the return echoes (or with electronic surveillance (ES) systems passively listening for target emissions). Radar waves, like all waves, reflect (or re-radiate) when encountering a boundary between two media. A boundary such as that between a metal and free space will reflect essentially all of the pulse, while a boundary between free space and a material with an electromagnetic impedance near that of free space (377 ohms) will reflect very little. The shaping, spacing and material of these boundaries, as well as the size of the aircraft and its boundaries relative to the radar wavelength, determine how the wave is reflected. Of interest is the magnitude of the reflected pulse in the direction of the receiving antenna, known as the radar echo or signal. The magnitude of the echo is directly proportional to the aircraft RCS.

1. RCS Shape (Magnitude and Azimuth)

Different shapes reflect waves differently. In descending order, the strongest magnitude reflections come from trihedral corners, dihedral corners, flat plates, cylinders, spheres, straight edges normal to the incident wave, curved edges normal to the wave, cones and ogives (Kopp, 1996). The RCS of an aircraft is actually the result of the vector/phase sum of the reflections, or echoes, from all the scattering surfaces the incident wave encounters. As such, the RCS changes dramatically with azimuth and the frequency of the incident wave. The result is a starburst pattern, shown in Figure III-1, that dramatically illustrates the scintillation produced by small changes in azimuth.

The RCS presented in Figure III-1 is much too complex for efficient modeling, therefore, several simplifications are made to make it easier to analyze. The most basic simplification is to represent the RCS with a circle of constant amplitude, known as a “fuzzball.”

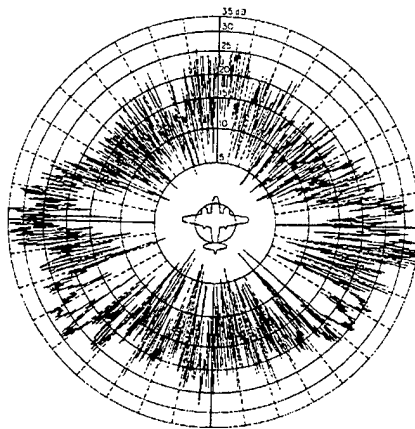


Figure III-1: Typical Aircraft RCS (after Skolnik)

2. How RCS is Reduced

A large part of reducing an aircraft's RCS involves carefully managing the shape of all possible boundaries. Furthermore, the inclusion of special lossy coatings closely matching the dielectric constant of free space help to absorb incident energy rather than reflect it. Obviously, the most effective way to reduce the RCS of an aircraft is to provide structural input early in the design phase. Unfortunately, the addition of coatings to a mature design is often likely to provide only moderate reductions at a high weight and cost penalty.

Signature reduction is most effective in typical combat situations when applied to the forward quarter of an aircraft ($\pm 60^\circ$ of the nose). This is due to the fact that prosecuting a forward quarter attack provides the threat system with favorable Doppler as well as increasing signal strength as the aircraft closes on the threat emitter. The beams and rear quarter are less critical due to the reduced Doppler in the beams and a combination of missile kinematics and the weakening signal strength of an opening target in the rear. The simplified RCS of an aircraft with this type of signature often resembles a "pacman," as seen in Figure III-2.

Reduced RCS on the nose



Figure III-2: Simplified RCS with Forward Quarter Reductions

To achieve true stealth, an aircraft must have a reduced RCS when viewed from any direction. However, an aircraft must have some edges, corners, and joints, making it very difficult to significantly reduce the RCS from all aspects. Therefore, edges, corners, and joints are all aligned to focus the RCS in two axes, comprising 4 directions or “lobes.” The resulting “X” shaped RCS is shown in Figure III-3.

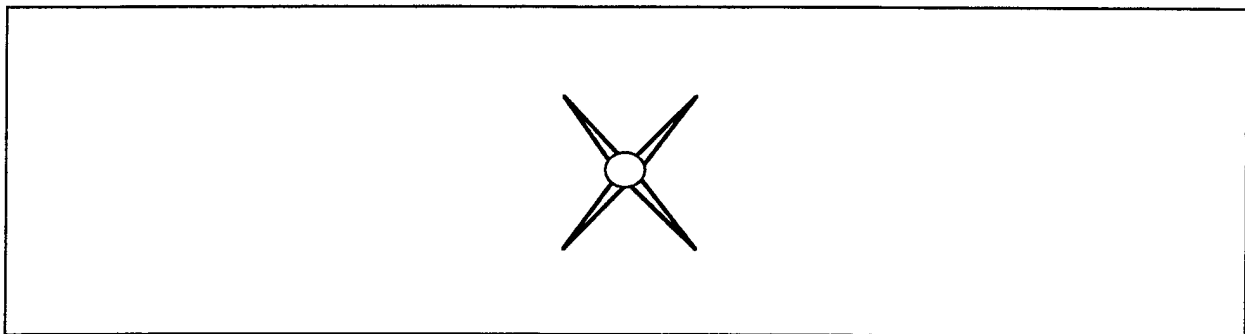


Figure III-3: RCS with All Aspect Reductions

B. RADAR DETECTION AND THE EFFECT OF SIGNATURE REDUCTION

Signature reduction has a dramatic affect on survivability. Reducing the RCS of the aircraft reduces the probability of detection, tracking, and missile launch at any given range. This leads to a reduction in the aircraft’s exposure to the threat by reducing the time spent in a threat envelope. All of these effects serve to increase the P_s of the aircraft.

A study of how RCS reduction affects survivability must begin with a discussion of how radar works. Monostatic radar determines the location of objects by transmitting electromagnetic pulses from an antenna, and then “listening” for the echo with the same (collocated) antenna. If the pulse is transmitted from an isotropic antenna (one which transmits uniformly in all directions), the power density in the pulse a distance R from the radar is calculated using eq. (III-1),

$$\text{Isotropic power density at range } R = \frac{P_t}{4\pi R^2} \quad [\text{W m}^{-2}] \quad (\text{III-1})$$

where P_t is the radar transmitter power in watts, and R is distance from the radar in meters. The $4\pi R^2$ in the denominator accounts for the decrease in signal strength as the power is spread spherically, and is termed the “spreading loss.” Radars employ directive antennas, which serve to

focus the power in a specific direction. The measure of how well the antenna functions in this capacity is termed the antenna gain, defined as the power density spread in the desired direction divided by the power density that would have been radiated by an isotropic antenna. To account for this gain, eq. (III-1) is multiplied by the radar antenna's transmitter gain, G_t . Incidentally, the radar power times the antenna gain is termed the effective radiated power (ERP).

If the transmitted power density impinges on an aircraft or other target, some of the power is reflected toward the radar receiver. The amount of power reflected is a direct function of the RCS, denoted σ , and is highly dependent on aspect angle, frequency, and aircraft scattering surfaces. RCS is defined as "the fictional area intercepting that amount of power, which, when scattered equally in all directions, produces an echo at the radar equal to that from the target" (Skolnick, 1980). The echo also suffers from spreading loss on the return path to the radar, where it is detected based on the effective area of the antenna, A_e . The resulting equation for echo power, S , is provided as Eq. (III-2).

$$\text{Power received } S = \frac{P_t G_t}{4\pi R^2} \times \frac{\sigma}{4\pi R^2} \times A_e \quad (\text{III-2})$$

Eq. (III-3) is the relationship between the effective area of an antenna A_e in square meters, and its gain, G .

$$A_e = \frac{G\lambda^2}{4\pi} \quad (\text{III-3})$$

where λ is the wavelength in meters. For the monostatic radar, which receives and transmits using the same antenna, substituting A , given by eq. (III-3), into eq. (III-2) results in eq. (III-4),

$$S = \frac{P_t G_t^2 \lambda^2 \sigma}{(4\pi)^3 R^4} \quad (\text{III-4})$$

which shows the direct relationship between the received echo signal power and the RCS. Figure III-4 is a graphical depiction of a typical two-way path for a radar transmission.

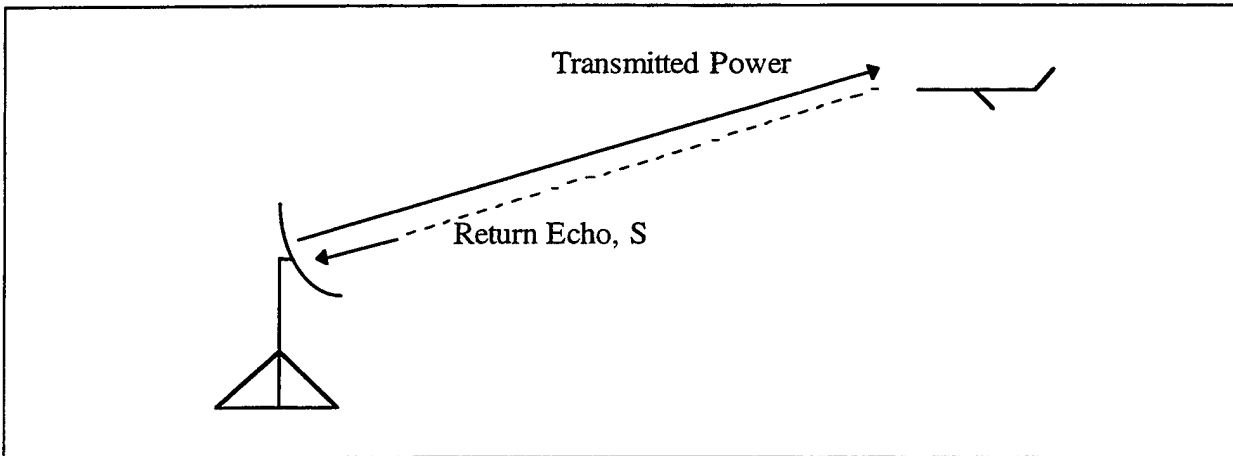


Figure III-4: Typical Radar Transmission Path

The maximum range at which detection by threat radar occurs (excluding noise and losses) can be computed by solving for R in eq. (III-4). The result is eq. (III-5), where S_{\min} represents the minimum signal power received that will result in detection.

$$R_{\max \text{ detection}} = \sqrt[4]{\frac{P_t G_t^2 \lambda^2 \sigma}{(4\pi)^3 S_{\min}}} \quad (\text{III-5})$$

The noise power present in the receiver bandwidth must be taken into account, as well as system losses such as plumbing, scanning, beam-shaping, collapsing, limiting, field degradation, etc., when estimating detection ranges. Losses are typically lumped together and included as the term L in the denominator. This loss factor is evaluated for each type radar system and can be used to evaluate design efficiency. The noise power present in the frequency band processed by the receiver is calculated according to eq. (III-6),

$$N = kT_s B_r = k(T_a + T_e)B_r \quad (\text{III-6})$$

where k is Boltzmann's constant ($1.38 \times 10^{-23} \text{ J/}^\circ\text{K}$), T_s is the equivalent noise temperature of the entire system, and B_r is the noise bandwidth of the receiver. The equivalent noise temperature of the system can be broken down into the antenna noise temperature, T_a and the equipment noise temperature, T_e . The noise bandwidth of the receiver is approximately equal to the IF bandwidth of the radar, which is in turn approximately equal to the reciprocal of the pulse width for an optimum matched filter IF bandwidth.

The antenna noise temperature, T_a , accounts for the noise power from all sources "upstream" of the antenna output terminals. Sources of this noise include the sun and moon (atmospheric noise), radome, antenna, and waveguides. Obviously, the antenna noise power present depends largely on the noise background in the direction the beam is pointing. The equipment noise takes into account the thermal noise produced in the receiver, and is commonly defined using eq. (III-7),

$$T_e = (F_n - 1)T_0 \quad (\text{III - 7})$$

where F_n is the receiver noise figure, and T_0 is the ambient noise temperature (290°K). The receiver noise figure is a measure of how much the input signal-to-noise ratio is degraded and is commonly equated to the ratio of the noise output of the actual receiver compared to the noise output of an ideal receiver. It is often assumed that $T_a = T_0$, in which case the noise power present in the receiver is calculated using eq. (III-8).

$$N = kT_0B_rF_n \quad (\text{III - 8})$$

The minimum received signal power that results in detection depends on many things. In order for a signal to be detected, it must exceed a preset threshold relative to the random background noise. The amplitude of the background noise at any instant in time will vary in a Gaussian manner. This distributed noise will have an average amplitude about which the instantaneous amplitudes are distributed. Figure III-5 is a good depiction of this.

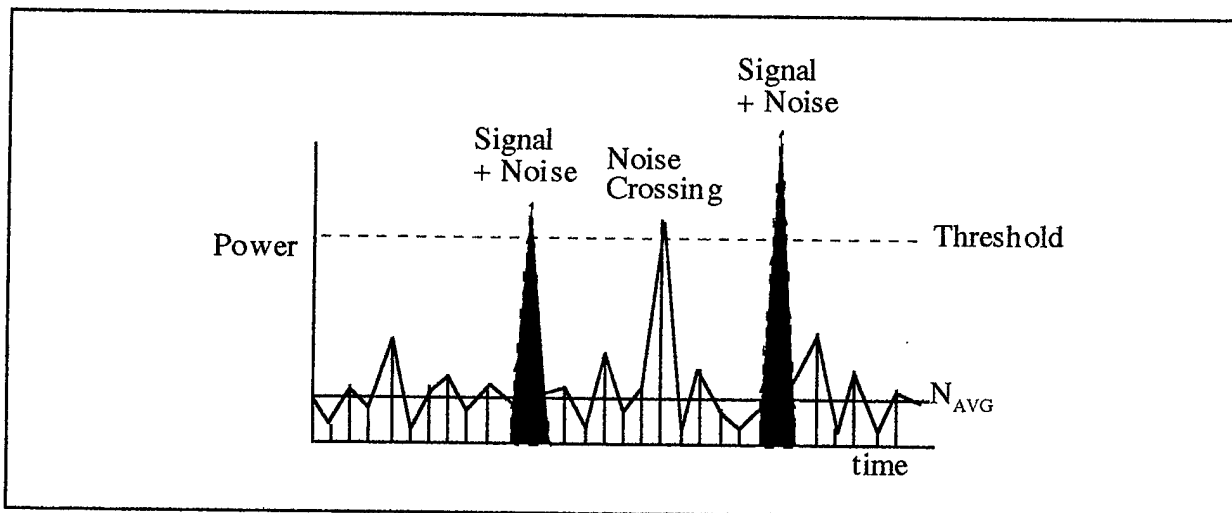


Figure III-5: Signal to Noise Threshold

The radar designer sets a threshold to limit the number of noise spikes above that threshold to a predetermined rate, called the false alarm rate. The setting of this threshold involves a trade off between an acceptable false alarm rate and the desired probability of detection. Increasing the threshold decreases both the false alarm rate and the probability of detection, and vice versa. It has been experimentally shown that reasonable false alarm rates and probabilities of detection for radars utilizing automatic detection logic result in required signal-to-noise, $(S/N)_{det}$, ratios of 10-25 (10-14 dB). For operator-in-the-loop systems, the required signal-to-noise ratio drops to 6-10 (8-10 dB), depending on operator proficiency (Levien, 1997).

The effect of noise and the threshold signal-to-noise ratio on the ability of the radar to process a signal is accounted for by multiplying and dividing S_{min} by the noise power, given by eq. (III-8). The result is eq. (III-9),

$$S_{min} = kT_0 B_r F_n (S/N)_{det} \quad (III-9)$$

where S/N_{det} is the minimum signal-to-noise ratio required by the threat radar to detect a target against the noise background. Substituting S_{min} given by eq. (III-9) into eq. (III-5) and including the loss factor L in the denominator results in eq. (III-10), the more familiar form of the radar range equation.

$$R_{max} = \sqrt{\frac{P_t G_t^2 \lambda^2 \sigma}{(4\pi)^3 L k T_0 B_r F_n (S/N)_{det}}} \quad (III-10)$$

Decreasing any of the terms in the numerator or increasing any of the terms in the denominator will reduce the maximum detection range. The only factor aircraft designers have control over is obviously the RCS of the platform. Thus, reducing RCS is the major way designers try to reduce susceptibility to radar guided threats.

Equation (III-10) applies only to a single pulse from a radar that has echo power S given by eq. (III-4). As a radar scans across a target, it receives a return echo on each successive pulse. By integrating the signal power from all these echo pulses, the receiver adds the signals linearly to get a much stronger resultant signal. The noise, on the other hand, does not add linearly. As discussed earlier, noise varies randomly in amplitude. It also varies randomly in phase. Thus, unlike the coherent radar signal, the incoherent noise adds vectorially as seen in Figure III-6.

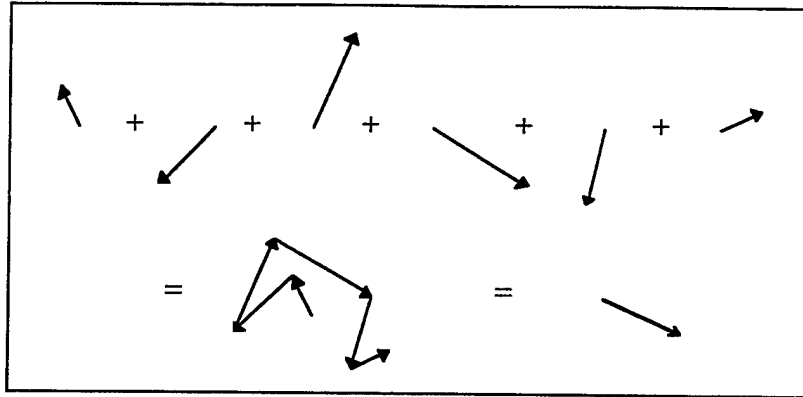


Figure III-6: Noise Added Vectorially

Perfect integration, also called predetection integration, adds up all the return echoes to get a combined signal strength. The number of pulses impacting a target per scan is given by eq. (III-11),

$$N = \frac{\theta \cdot F_p}{\omega} \quad (\text{III-11})$$

where N is the number of pulses per scan, θ is the antenna beamwidth in degrees, F_p is the pulse repetition frequency, or PRF, in pulses per second, and ω is the antenna scan rate in degrees per second. Unfortunately, a perfect integrator is difficult to implement and seldom used. Analysis of data presented by Skolnik demonstrates a simple relationship between the integration improvement factor, $I(N)$, and the number of pulses on a target, N . This relationship is presented in eq. (III-12) and holds for postdetection integration, which is easier to accomplish and more commonly used.

$$I(N) = N^{0.8} = \left(\frac{\theta F_p}{\omega} \right)^{0.8} \quad (\text{III-12})$$

This integration improvement factor measures the magnitude of the power S , given by the right hand side of eq. (III-4). Thus, eq. (III-10) becomes eq. (III-13),

$$R_{\max} = \sqrt[4]{\frac{P_t G_t^2 \lambda^2 \sigma}{(4\pi)^3 L k T_0 B_r F_n (S/N)_{\text{det}}} \cdot \left(\frac{\theta F_p}{\omega} \right)^{0.8}} \quad (\text{III-13})$$

where S/N_{det} still represents the minimum signal-to-noise ratio required by the threat radar to detect a target against the noise background.

Given that reducing RCS is to be used to reduce susceptibility, how much should the RCS be reduced to avoid detection until a given range? The RCS required to avoid detection until a given range, R_{max} , is solved for by rearranging the preceding equation, which yields eq. (III-14).

$$\sigma = \frac{R_{max}^4 (4\pi)^3 L k T_0 B_r F_n (S/N)_{det}}{P_t G_t^2 \lambda^2} \cdot \left(\frac{\omega}{\theta F_p} \right)^{0.8} \quad (III-14)$$

Data from unclassified sources are not typically available for all the parameters in eqs. (III-13 and 14). Specifically, antenna gain is rarely presented in unclassified documents. To permit an analysis using unclassified data presented, two methods of estimating antenna gain are presented. A good estimate of the gain of a circular aperture antenna at frequencies near 10 GHz is given by eq. (III-15),

$$G_t = d^2 \eta \quad (III-15)$$

where d is the antenna diameter in centimeters and η is the aperture efficiency (typically 70%) (Stimson, 1983). This is extremely useful for airborne fire control radars which operate near 10 GHz. Another convenient approximation involves the beamwidth of the radar, which is often published openly. The gain for a circular parabolic antenna can be approximated using eq. (III-16),

$$G_t \approx \frac{26,000}{\theta \phi} \quad (III-16)$$

where θ and ϕ are the 3 dB beamwidth, in degrees, in the two planes of interest (Stutzman and Thiele, 1981).

In order to use eq. (III-14) as a means of using unclassified data to calculate how small the RCS must be in order to inhibit detection until a certain range, some representative values for the other variables must be provided. Widely published unclassified data, as well as some engineering estimates, were used to create a list of representative values, included as Table III-1.

Table III-1: Typical Radar Parameters

Parameters	A-A	Strike
P_t (kW)	5	1,500
B_r (kHz)	7.5	1,250
F_n	7	6
L	30	6
S/N_{det}	20	10
f (GHz)	10	5
λ (m)	0.03	0.06
F_p (Hz)	1,500	1,140
ω (deg/sec)	80	120
θ (degrees)	2.5	1.5
η	0.7	NA
d (cm)	71	NA
Gain	3,529 (eq. III-15)	11,556 (eq. III-16)
σ (m^2)	0.31	8.66E-06

In accordance with the mission threat analysis performed previously, the aircraft is required to avoid detection until 35 km (19 nm) for the air-to-air mission against a typical airborne threat radar (the Mig-29 Slotback radar), and until 11 km (6 nm) for the Strike mission against a common ground based radar (the SA-2E Fansong radar). Meters were chosen as the unit of length since radar data are typically presented in those units, although nautical miles are more significant tactically.

Using these data and eq. (III-14), Figures III-7 and III-8 were generated, which plot RCS versus detection range for the threat radars in the air-to-air and strike scenarios, respectively, where the tick on the range axis indicates the requirements of the mission threat analysis.

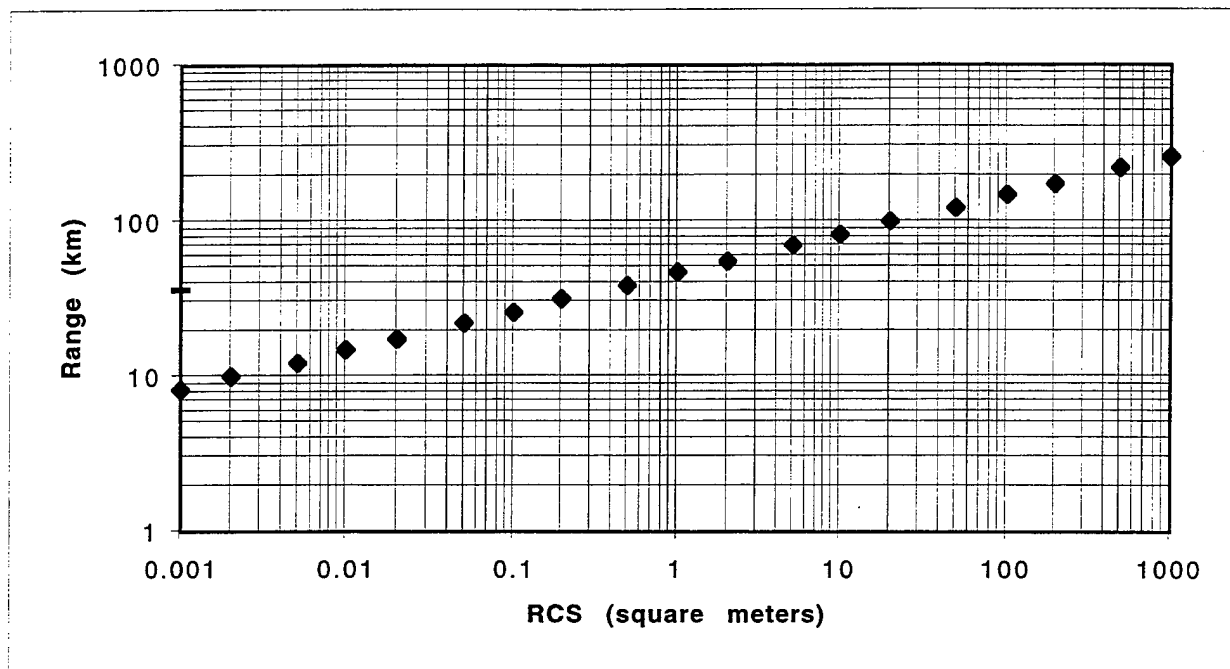


Figure III-7: RCS vs. Range for Air-to-Air Radar (S/N = 20)

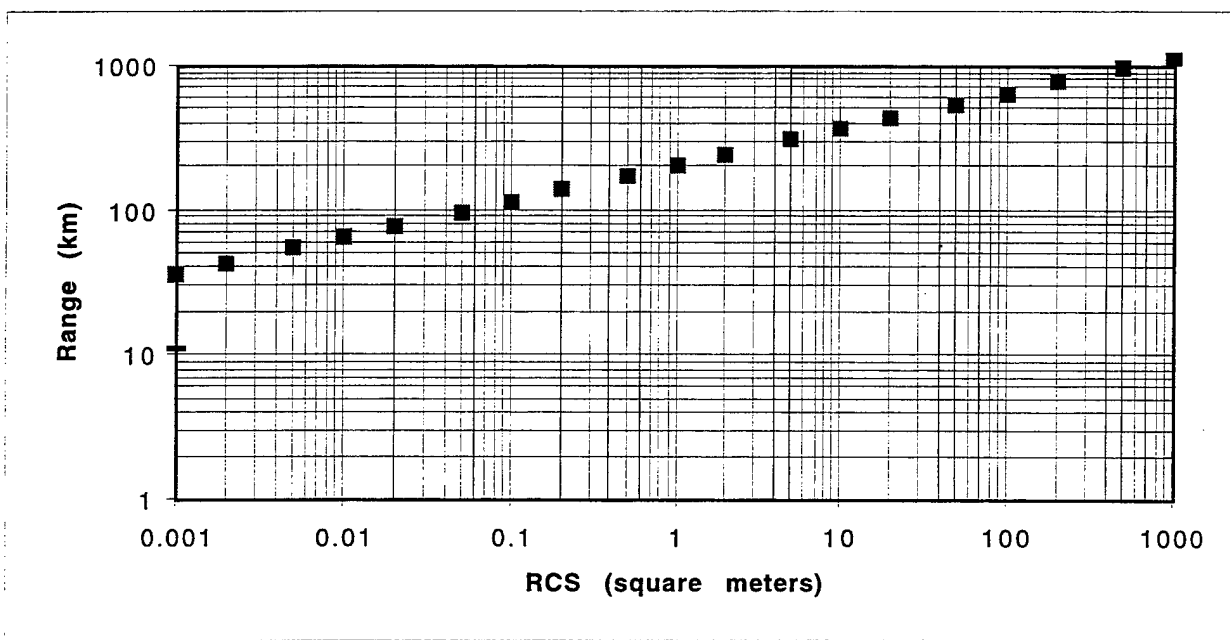


Figure III-8: RCS vs. Range for Strike Radar (S/N = 10)

C. COUNTERING SIGNATURE REDUCTION

With so much emphasis on reducing aircraft RCS, we must assume that a strong emphasis will also be placed on countering stealth technology. Short of fielding and integrating huge numbers of tracking radars to achieve sufficient radar density to maintain a track, one method of countering stealth is to use radars with lower frequency and/or wider bandwidth. These have great potential, but current authors indicate that they are incapable of providing fire control data for weapons launch. Another recent attempt at countering stealth involved the discovery of the "radar hole" left by such aircraft. A stealth aircraft attempts to focus whatever reflected electro-magnetic waves it can't absorb in directions deemed to be tactically less threatening, typically 45 - 60 degrees off the nose. A byproduct of this is that the aircraft also reduces the amount of "clutter" the radar receives in the direction of the aircraft. If the lack of radar return clutter could be tracked effectively, it would render stealth incapable of providing the required tactical advantage. A third possible solution to the stealth threat involves the use of bi-static radars (radars that employ different antennas to transmit and receive) with widely separated antennas. In theory, a bi-static radar could disperse receive antennas to take advantage of the focused radar return of stealth aircraft to generate fire control solutions. Nevertheless, every reduction in RCS increases the enemy's cost of admission to the next conflict.

The end result of effective solutions to the stealth problem, in any event, would be a lessening of the effectiveness of RCS reductions and a corresponding stronger need for EA capabilities. For the purposes of this report, stealth will be considered to be effective. A lessening of its effectiveness could be treated as a larger RCS circle or ellipse, leading to a need for more powerful EA capabilities.

IV. ONBOARD ELECTRONIC ATTACK AND SUSCEPTIBILITY REDUCTION

A. NOISE JAMMING AND DECEIVING

Electronic warfare is made up of three essential elements, Electronic Surveillance (ES), Electronic Attack (EA), and Electronic Protection (EP). Electronic Surveillance deals with intercepting and analyzing electromagnetic emissions in order to develop a better understanding of enemy capabilities and to determine an appropriate response. Electronic Attack, formerly called electronic countermeasures (ECM), encompasses all methods of denying the use of the electromagnetic spectrum to the enemy. Electronic Protection, formerly called electronic counter-countermeasures (ECCM), describes any action taken to prevent the enemy from denying the use of the electromagnetic spectrum by friendly forces.

Two important tenets of EA designed to deny the enemy's use of radar (and communications) are noise jamming and deceiving. For noise jamming and deceiving to be effective, it has been experimentally demonstrated that the jammer power must exceed some threshold related to the echo signal power. This threshold is typically referred to as the jamming to signal ratio required for effectiveness, or $(J/S)_{req'd}$. The development of this ratio starts with the strength of the return "echo" received by the victim radar previously defined as follows in eq. (III-4):

$$S = \frac{P_t G_t^2 \lambda^2 \sigma}{(4\pi)^3 R^4} \quad (\text{III - 4})$$

The strength of the return echo suffers from a 2-way spreading loss as seen by the factor of R^4 in the denominator. The jammer power, on the other hand, only suffers from a 1-way spreading loss. If the effective radiated power (ERP) of the jammer is given by $P_j G_j$, where P_j is the jammer transmitter power and G_j is the jammer antenna gain, then the jammer power received by the victim radar receiver, $P_{r/j}$, is given by eq. (IV-1),

$$P_{r/j} = J = \left(\frac{P_j G_j}{4\pi R^2} \right) \times \left(\frac{\lambda^2 G_t}{4\pi} \right) = \frac{P_j G_j G_t \lambda^2}{(4\pi R)^2} \quad (\text{IV - 1})$$

Unfortunately, the polarization of the jammer is rarely the same as that of the radar. Jammers are typically circularly (or slant) polarized in order to maintain effectiveness against both horizontally and vertically polarized radars. (If the jammer were horizontally polarized and the radar were vertically polarized, theoretically, none of the jammer power would get to the receiver. In reality, approximately 1% of the jammer power gets to the receiver.) This results in the radar “filtering out” a significant amount of the jammer power due to the polarization mismatch. To account for this polarization loss, the “ L_p ” factor is added to the denominator of eq. (IV-1), as seen in eq. (IV-2).

$$J = \frac{P_j G_j G_t \lambda^2}{(4\pi R)^2 L_p} \quad (IV-2)$$

A typical value for L_p is 2, representing a polarization loss of 3 dB, or half the power.

The J/S ratio can be derived by dividing the jammer power at the victim receiver (eq. IV-2) by the signal power at the victim receiver (eq. III-4). The result is eq. (IV-3).

$$\left(\frac{J}{S}\right) = \frac{P_j G_j R^2 4\pi}{P_t G_t \sigma L_p} \quad (IV-3)$$

There are numerous different jamming techniques available to the countermeasures designer. Different techniques generally require different J/S ratios to be effective. Of interest to the countermeasures designer is the Jammer Effective Radiated Power (JERP) required to equal the $(J/S)_{req'd}$, for a given technique, at a specific range. Solving eq. (IV-3) for JERP ($P_j G_j$), yields,

$$P_j G_j = \frac{\left(\frac{J}{S}\right)_{req'd} P_t G_t \sigma L_p}{R^2 4\pi} \quad (IV-4)$$

Thus, the JERP required to effectively defeat a target radar at a specific range is a function of the $(J/S)_{req'd}$ for the jamming technique being implemented, the ERP of the radar being jammed, and the RCS of the aircraft. Of prime importance when choosing which jamming techniques to implement is an understanding of the technique, as well as the $(J/S)_{req'd}$ for that technique to be effective. A short, unclassified, description of several common EA techniques, as well as their $(J/S)_{req'd}$, is presented below.

1. Noise Jamming

Noise jamming involves the injection of "noise" into the victim radar receiver. If the noise jamming is strong enough, it raises the average noise power in the receiver, thereby degrading the $S/(N+J)$ ratio in the receiver to a low enough level that the signal is obscured. The jammer power must at least equal the signal power in the receiver in order to obscure the signal. The jammer power must be at least 1-4 times greater than the signal power ($J/S = 0-6$ dB) to be effective (Schleher, 1986). Figure IV-1 shows the combination of jammer power, noise power and signal power.

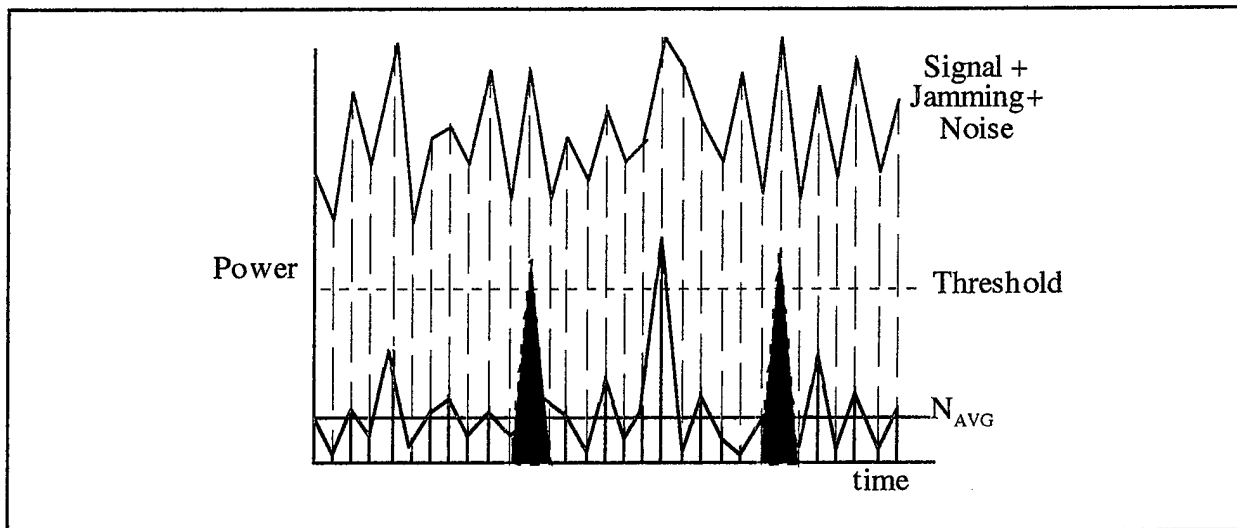


Figure IV-1: Signal + Noise + Jamming

There are two general classifications of noise jamming based on the bandwidth ratio, B_j/B_r . If the jammer bandwidth is essentially equal to the receiver bandwidth (the bandwidth ratio is low) the jamming is termed "spot" noise jamming. Thus, eq. (IV-4) holds for spot noise jamming, if the bandwidth over which the jammer power is spread exactly equals the instantaneous bandwidth of the radar receiver. If, on the other hand, the jammer bandwidth is significantly larger than the receiver bandwidth (the bandwidth ratio is high), the jamming is termed "barrage" noise jamming. Spot jamming is obviously the most efficient form of noise jamming in terms of jammer power required, but the advent of frequency agile radars has generally forced a transition to barrage jamming, or frequency following jamming.

Frequency agile radars transmit over numerous frequencies within a defined operating range. One series of pulses may be transmitted at one frequency, and the next series can be transmitted at a frequency several hundred megahertz different from the first. In addition to

frequency, the radar may alter the PRF and pulse width from one transmission to the next, which changes the instantaneous bandwidth as shown in the previous chapter. The receiver processing the radar return has the additional advantage of knowing the bandwidth of the transmitted waveform. This bandwidth is expanded slightly by the receiver (to account for Doppler shifts) and a band pass filter is employed to exclude all the energy (noise, jamming, and deception) that does not occur in that bandwidth. The jammer, on the other hand, will never know for certain exactly where on the frequency spectrum the radar may transmit next (assuming the frequency hopping algorithm is not readily predictable), and must spread the jammer power over the entire range of frequencies over which the radar is likely to operate. Thus, the difference in bandwidths must be taken into account in eqs. (IV-2) and (IV-4). Eq. (IV-5) shows how the received signal is processed over the instantaneous bandwidth of the receiver only, whereas the noise jammer power is spread over the jammer operating bandwidth B_j .

$$J = \frac{P_j G_j G_t \lambda^2 B_r}{(4\pi R)^2 B_j p} \quad (IV - 5)$$

Dividing eq. (IV-5) by the return radar signal as before, and again solving for the noise jammer ERP results in eq. (IV-6).

$$P_j G_j = \frac{\left(\frac{J}{S}\right)_{\text{Req'd}} P_t G_t B_j \sigma p}{B_r R^2 4\pi} \quad (IV - 6)$$

Furthermore, the noise jammer power, like the noise it seeks to replicate, will not be integrated in the receiver, whereas the signal power will benefit from the integration improvement factor, I , given by eq. (III-8). This is taken into account in eq. (IV-7).

$$P_j G_j = \frac{\left(\frac{J}{S}\right)_{\text{Req'd}} P_t G_t B_j \sigma p}{B_r R^2 4\pi} \times \left(\frac{\theta F_p}{\omega}\right)^{0.8} \quad (IV - 7)$$

Thus, the main goal of a frequency agile radar is to force the noise jammer into less efficient barrage jamming by spreading radar transmissions over a wide frequency band. An additional benefit is that by spreading the transmissions over a wide frequency band, the frequency agile radar reduces the probability of detection by ES systems.

2. Range Gate Pull Off (RGPO)

Range Gate Pull Off (RGPO) is the first of several deceptive techniques presented in this report. Deceptive jamming differs from noise jamming in that there is typically no bandwidth differential. Furthermore, since the jammer waveform strives to be nearly identical to the signal waveform, it will be integrated and will suffer losses much like the signal waveform. The integration and loss factors for the jammer waveform will not exactly equal the integration and loss factors for the signal waveform, but will be approximated as such in this report. Therefore, the J/S ratio will be the same for many integrated pulses as it is for a single pulse, given by eq. (IV-4).

RGPO is effective against pulsed radars utilizing automatic gain control (AGC). Pulse radars determine target range by transmitting pulses and determining the time required for the echo to return. The range is equal to the speed of light times the time delay divided by 2 to account for the 2-way trip. Once the radar receives an echo, it establishes "range gates" around the time it expects the next echo to arrive. Typically, this involves straddling the expected return time with an early and a late gate. The jammer observes the pulse, and immediately transmits an identical cover pulse. The strength of the cover pulse is gradually increased until it eventually forces the radar's AGC to lower its sensitivity to the actual skin return of the aircraft. Once this occurs, the jammer then walks the range gates off the aircraft by delaying the transmitted pulse an ever increasing amount. The rate at which the time delay increases must be representative of typical target maneuvers, i.e. increasing the delay at a rate corresponding to a 20-g turn might trigger a logic loop which identifies the deception. Once the deception is sufficient, the jamming ceases and the radar is forced to re-acquire the aircraft. The jammer power at the victim receiver must be 1-4 times greater than the signal power ($J/S = 0-6$ dB) for this technique to be effective (Schleher, 1986).

Another related deception technique is range gate pull in (RGPI). Due to the use of time delayed transmissions, the RGPO technique can only deceive the radar into thinking the target is farther away. If the radar uses an easily predictable pulse repetition interval (PRI), then the time of arrival of the next pulse can be anticipated. If the jammer can capture the range gates and transmit a stronger pulse ahead of the return echo, the range gates can be walked in toward the radar. A third related option is "smart" noise jamming, in which the jammer acknowledges the unpredictable, ever changing PRI and transmits a relatively long burst of noise timed after the preceding pulse and of long enough duration to cover all possible PRI's of the following pulse.

3. Velocity Gate Pull Off (VGPO)

Velocity Gate Pull Off (VGPO) is a deception technique that is effective against Continuous wave (CW) and pulse Doppler (PD) radars. CW and PD radars use the Doppler frequency shift of the target to set up velocity gates in much the same way pulse radars use range gates. Due to the dynamics of an encounter between an aircraft and a threat radar, the closure rate (and Doppler frequency shift) may change rapidly. In addition, the return signal strength can fluctuate dramatically as the target aspect (and RCS) changes. Thus, the jammer must transmit a much stronger signal at the same frequency as the incident radar signal to capture the velocity gate. If the jammer and the aircraft move together (always the case with onboard jamming, but not necessarily so with a towed transmitter while maneuvering) the return signal from the aircraft and the jammer signal will be shifted equally. The jammer signal is then increased in frequency and walked off in velocity. As in RGPO, the rate at which the jammer frequency is increased must be representative of typical aircraft maneuvers. The jammer power at the victim receiver must also be 1-4 times greater than the signal power ($J/S = 0-6$ dB) for this technique to be effective (Schleher, 1986).

4. Inverse Gain Scan

Inverse gain scan is a deception technique with good effectiveness against Conical scan (Conscan) radars. Conscan radars track targets by nutating a feed about the center of their antenna, thereby creating a pencil beam that rotates about the antenna boresight. If the target resides along the antenna boresight, the return signal will be constant. If the target being tracked does not lie on the antenna boresight, the return signal will be stronger in the direction of the target offset. Furthermore, the amplitude of the return signal will fluctuate at the same rate at which the antenna feed is being nutated, as shown in Figure IV-2.

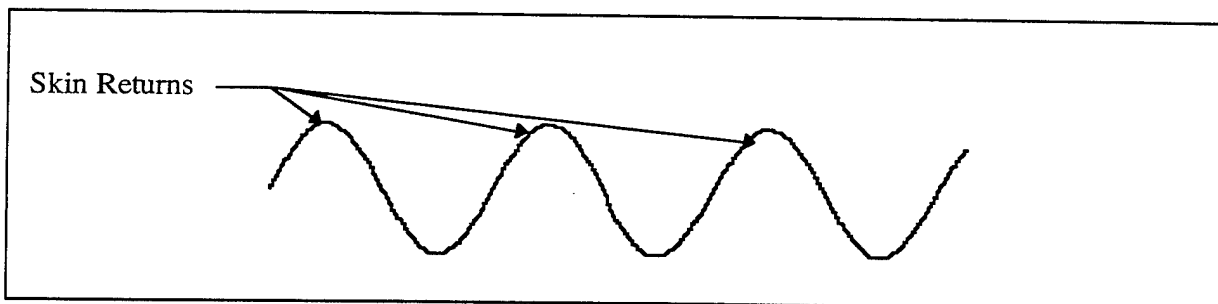


Figure IV-2: Conscan Radar Return Fluctuating Due to Target Presence

Target offset can then be determined based on the difference in the relative signal strength of the fluctuating return signal. The antenna is then repositioned in that direction until the return signal amplitude becomes relatively constant again.

The aircraft being tracked can also detect the scan modulation of the tracking radar. An inverse gain jammer might then inject high power pulses 180 degrees out of phase with the skin return based on the scan rate as shown in Figure IV-3.

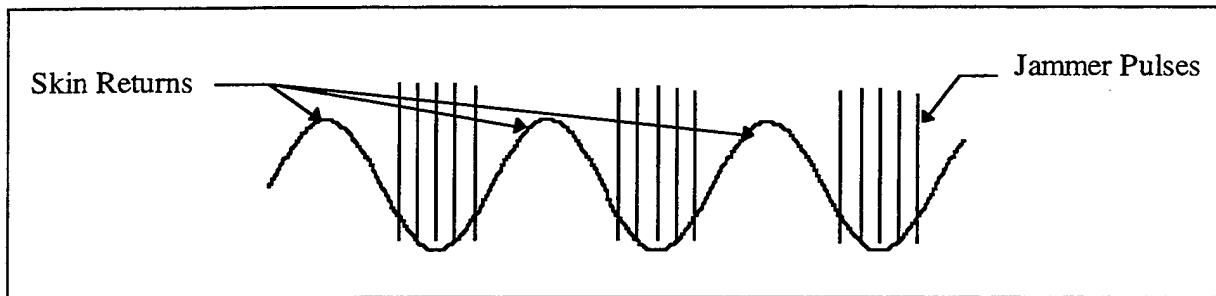


Figure IV-3: Conscan Radar Return Plus Inverse Gain Jamming

The result of this jamming would be that the conscan antenna is commanded in the opposite direction of the target offset. Unfortunately, the jammer power at the victim receiver must be 10-300 times greater than the signal power ($J/S = 10-25$ dB) for this technique to be effective (Schleher, 1986).

5. Cross Eye

Cross eye jamming is an implementation of dual coherent source jamming that enjoys good effectiveness against monopulse radars. This deception technique employs dual, separate, repeater paths to generate a "null" at the victim receiver in the direction of the jammer. Each repeater path retransmits a received signal from the position at which the other has received it. The repeater path lengths must be electrically identical to maintain the proper phase relationship. Additionally, one of the paths must contain a phase shifter to ensure that the two retransmissions add destructively at the victim receiver to create a null. If this null is strong enough, it will cover up the skin return of the aircraft. Figure IV-4 shows a typical cross eye relationship.

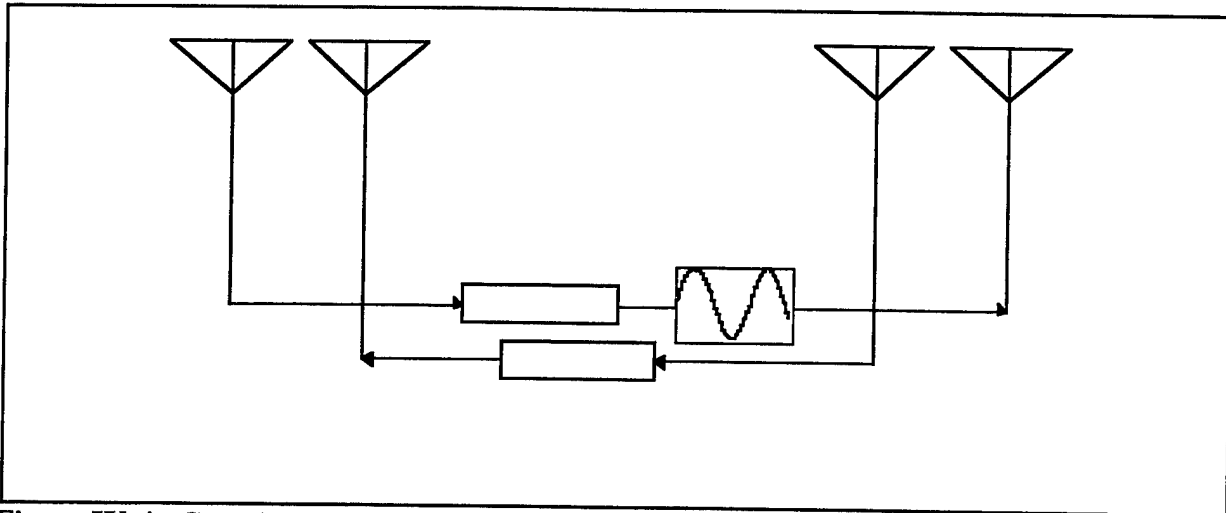


Figure IV-4: Cross Eye Repeater Jamming Implementation

The effectiveness of this technique is limited by the spacing between the receiving antenna and the transmitting antenna, which is called the baseline. Current implementations involve wingtip installations and are baseline limited by the overall aircraft wingspan. Towed decoy implementations would present a much greater potential baseline, at the expense of limited effectiveness on the nose and tail. Unfortunately, the jammer power at the victim receiver must be approximately 100 times greater than the signal power ($J/S = 20$ dB) for this technique to be effective (Schleher, 1986). Furthermore, the actual jammer power required varies with the baseline length.

6. Cross Polarization

Cross polarization jamming is a deception technique that is effective against some monopulse radars. Monopulse radars use multiple lobes simultaneously to determine the angular position of a target by comparing the signal strength between lobes. When a parabolic reflector is used in the implementation, the antenna naturally radiates a small portion of the power orthogonal to the primary polarization. This polarization skewing is accounted for when processing the received echo. The cross polarization jammer determines the polarization of the incoming signal, and retransmits a signal whose polarization is orthogonal to the incoming signal. If the jammer power density at the radar antenna is at least 100 times greater than the signal power density (to account for the polarization mismatch which attenuates 99% of the jammer power density), the jammer power will be of the same order as the signal power at the antenna terminals. This additional power will induce an azimuth or elevation error in the monopulse radar in the same

manner that inverse gain affects conscan radars. This causes the monopulse radar to make a correction in a wrong direction, thereby walking the radar beam away from the aircraft. As stated earlier, the jammer power must be at least 100 times greater than the signal power ($J/S > 20$ dB) for this technique to be effective (Schleher, 1986).

B. JAMMING SUMMARY

Table IV-1 summarizes the representative jamming techniques presented above, the associated $(J/S)_{req'd}$ for each, and the intended victim radar types.

Table IV-1: Radar Jamming Techniques (after Schleher, 1986)

Jamming Technique	$(J/S)_{req}$	$(J/S)_{req}$ (dB)	Victim Radar Type
Noise	1-4	0-6	Pulse
RGPO	1-4	0-6	Pulse, Pulse Doppler
VGPO	1-4	0-6	CW, Pulse Doppler
Inverse Gain	10-300	10-25	Conscan, Angle Tracking, Lobing
Cross Eye	100	20	Monopulse
Cross Polarization	100-10,000	20-40	Monopulse

Modern self-protection jammers are capable of as many as several thousand watts JERP and utilize many techniques. The AN/ULQ-21 (V) Countermeasures Set is a modern, digital system used to simulate EA threats for testing and training requirements. Many of the techniques discussed above can be generated by the ULQ-21, as well as more current techniques. A partial list of ULQ-21 techniques is included as table IV-2.

A limitation of pure noise jamming, however, is susceptibility to track-on-jam/home-on-jam (TOJ/HOJ) systems. Thus, the ULQ-21 (and other modern jammers) uses coherent, smart noise jamming techniques. Furthermore, jamming is much more effective when several techniques are combined, particularly when range denial (noise jamming) and azimuth deception (cross polarization, etc.) are combined.

Table IV-2: Representative ULQ-21 Techniques

Jamming Technique
Noise (continuous, blinking, or swept)
Amplitude Modulation
Range Deception/RGPO
Velocity Deception/VGPO
Pseudo Random Noise
Doppler Noise
Non-Adaptive Cross Polarization
Cooperative Blink, AM (on/off)
Coherent RGPO
Coherent VGPO
Terrain Bounce

V. SURVIVABILITY ENHANCEMENT DUE TO COMBINED SIGNATURE REDUCTION AND ELECTRONIC ATTACK

A. SIGNATURE REDUCTION AND ELECTRONIC ATTACK COMBINED

The effect of combining signature reduction and electronic warfare capabilities is synergistic - the combined effect is greater than the sum of their individual contributions. A reduction in RCS enhances jamming because it reduces the skin return with which the jamming must compete. Analysis of this synergy starts with an understanding of a representative jamming scenario. A typical radar transmission involving jamming is shown in Figure V-1.

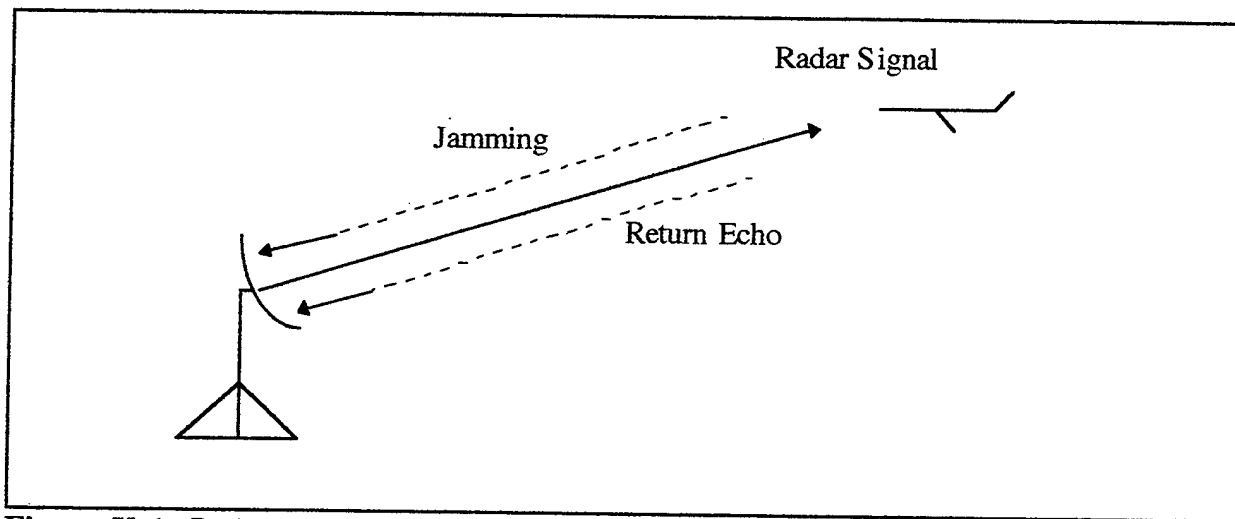


Figure V-1: Radar Path with Jamming

The jammer power adds to the noise power and return echo signal power at the receiver. Detection is accomplished if the signal power exceeds $(S/N)_{det}$ after being processed in the receiver. In the presence of jamming, this becomes the signal-to-interference (S/I) ratio, where interference is a combination of noise and jamming. Development of the signal-to-interference ratio is provided in eq. (V-1).

$$\left(\frac{S}{I}\right) = \frac{S}{N+J} = \frac{\frac{S}{N}}{1 + \frac{J}{N}} = \frac{\frac{S}{N}}{1 + \left(\frac{J}{S}\right)\left(\frac{S}{N}\right)} \quad (V-1)$$

A representative range of values for these variables are presented in table V-1. Note that numerically, (S/I) is essentially equal to (S/J), and that S/I is relatively insensitive to S/N variations.

Table V-1: Typical Ratio Values

S/N	J/S	S/I
8	4	0.242
10	4	0.244
20	4	0.247
8	10	0.099
10	10	0.099
20	10	0.100
8	100	0.010
10	100	0.010
20	100	0.010

Development of an equation which physically relates the ratio of the signal strength to the interference is more complex, and follows the developments in Chapter III. The "echo" signal power was previously defined as eq. (III-4).

$$S = \frac{P_t G_t^2 \lambda^2 \sigma}{(4\pi)^3 R^4} \quad (\text{III-4})$$

The signal-to-interference ratio is then given by eq. (V-2), where interference consists of jamming plus thermal noise, and system losses are accounted for with an L in the denominator.

$$\left(\frac{S}{I}\right) = \left(\frac{S}{N+J}\right) = \frac{P_t G_t^2 \lambda^2 \sigma}{(4\pi)^3 R^4 L (N+J)} \quad (\text{V-2})$$

Focusing initially on noise jamming, the receiver noise power, eq. (III-8), and the noise jammer power, eq. (IV-5), are incorporated into eq. (V-2), resulting in eq. (V-3).

$$\left(\frac{S}{I}\right) = \frac{P_t G_t^2 \lambda^2 \sigma}{(4\pi)^3 L R^4 \left(k T_0 B_r F_n + \frac{P_j G_j G_t \lambda^2 B_r}{(4\pi R)^2 B_j L_p} \right)} \quad (V-3)$$

In this form, eq. (V-3) applies to noise jamming against a single pulse. Multiplying the signal power (numerator) by the integration improvement factor, eq. (III-11), to account for the integration of numerous signal pulses (but not jammer power) results in eq. (V-4N),

$$\left(\frac{S}{I}\right) = \frac{P_t G_t^2 \lambda^2 \sigma}{(4\pi)^3 R^4 L \left(k T_0 B_r F_n + \frac{P_j G_j G_t \lambda^2 B_r}{(4\pi R)^2 B_j L_p} \right)} \times \left(\frac{\theta \cdot F_p}{\omega} \right)^{0.8} \quad (V-4N)$$

where the "N" suffix indicates applicability to noise jamming only.

An order of magnitude analysis of both the noise power at the receiver, eq. (III-6), and the jammer power at the receiver, eq. (IV-2), was conducted. The analysis was based on the air-to-air scenario and a self protection jammer with an ERP of 1 Watt. The comparison revealed that both power levels were similar orders of magnitude at approximately 30 nm. At close range, however, the jammer power rapidly exceeded the noise power.

Eq. (V-4N) can be adapted to deception techniques by applying the integration improvement factor to the jammer power in the denominator as well as the signal power in the numerator, eliminating the bandwidth ratio, and adding the loss factor L to the denominator. In this manner, everything except the noise benefits from pulse integration, as seen in eq. (V-4D),

$$\left(\frac{S}{I}\right) = \frac{P_t G_t^2 \lambda^2 \sigma}{(4\pi)^3 R^4 L \left(k T_0 B_r F_n + \left(\frac{P_j G_j G_t \lambda^2}{(4\pi R)^2 L_p} \right) \times \left(\frac{\theta \cdot F_p}{\omega} \right)^{0.8} \right)} \times \left(\frac{\theta \cdot F_p}{\omega} \right)^{0.8} \quad (V-4D)$$

where the "D" suffix indicates applicability to deception techniques only.

Analysis of eqs. (V-4N) and (V-4D) reveals five main sets of variables: R, JERP ($P_j G_j$), S/I, σ , and the radar unique parameters. The mission threat analyses serve to fix the radar unique parameters, leaving four remaining variables. In order to more fully understand these

relationships, it is useful to solve eqs. (V-4N) and (V-4D) in terms of each of the other three main variables. Solving for RCS, and JERP ($P_j G_j$), yields eqs. (V-5N), (V-5D), (V-6N), and (V-6D), respectively.

$$\sigma = \frac{\left(\frac{S}{I}\right)(4\pi)^3 R^4 L \left(k T_0 B_r F_n + \frac{P_j G_j G_t \lambda^2 B_r}{(4\pi R)^2 L_p B_j} \right)}{P_t G_t^2 \lambda^2} \times \left(\frac{\omega}{\theta F_p} \right)^{0.8} \quad (V-5N)$$

$$\sigma = \frac{\left(\frac{S}{I}\right)(4\pi)^3 R^4 L \left(k T_0 B_r F_n + \left(\frac{P_j G_j G_t \lambda^2}{(4\pi R)^2 L_p L} \right) \times \left(\frac{\theta F_p}{\omega} \right)^{0.8} \right)}{P_t G_t^2 \lambda^2} \times \left(\frac{\omega}{\theta F_p} \right)^{0.8} \quad (V-5D)$$

$$P_j G_j = \left(\frac{P_t G_t^2 \lambda^2 \sigma}{\left(\frac{S}{I}\right)(4\pi)^3 R^4 L} \left(\frac{\theta F_p}{\omega} \right)^{0.8} - k T_0 B_r F_n \right) \times \left(\frac{(4\pi R)^2 L_p B_j}{G_t \lambda^2 B_r} \right) \quad (V-6N)$$

$$P_j G_j = \left(\frac{P_t G_t^2 \lambda^2 \sigma}{\left(\frac{S}{I}\right)(4\pi)^3 R^4 L} \left(\frac{\theta F_p}{\omega} \right)^{0.8} - k T_0 B_r F_n \right) \times \left(\frac{(4\pi R)^2 L_p L}{G_t \lambda^2} \right) \times \left(\frac{\omega}{\theta F_p} \right)^{0.8} \quad (V-6D)$$

Solving for R is much more troublesome. Rewriting eqs. (V-4N) and (V-4D) in the form of a quadratic leads to eqs. (V-7N) and (V-7D).

$$R^4 \left(\frac{S}{I}\right) k T_0 B_r F_n + R^2 \left(\frac{S}{I}\right) \frac{P_j G_j G_t \lambda^2 B_r}{(4\pi)^2 B_j L_p} - \left(\frac{P_t G_t^2 \lambda^2 \sigma}{(4\pi)^3 L} \right) \times \left(\frac{\theta F_p}{\omega} \right)^{0.8} = 0 \quad (V-7N)$$

$$R^4 \left(\frac{S}{I}\right) k T_0 B_r F_n + R^2 \left(\frac{S}{I}\right) \times \left(\frac{P_j G_j G_t \lambda^2}{(4\pi)^2 L_p L} \right) \times \left(\frac{\theta F_p}{\omega} \right)^{0.8} - \left(\frac{P_t G_t^2 \lambda^2 \sigma}{(4\pi)^3 L} \right) \times \left(\frac{\theta F_p}{\omega} \right)^{0.8} = 0 \quad (V-7D)$$

Solving this quadratic equation for R^2 leads to eqs. (V-8N) and (V-8D).

$$R^2 = \frac{-\frac{P_j G_j G_t \lambda^2 B_r (S/I)}{(4\pi)^2 L_p B_j} + \sqrt{\left(\frac{P_j G_j G_t \lambda^2 B_r (S/I)}{(4\pi)^2 L_p B_j}\right)^2 + \frac{4(S/I) k T_0 B_r F_n P_t G_t^2 \lambda^2 \sigma \left(\frac{\theta F_p}{\omega}\right)^{0.8}}{(4\pi)^3 L}}}{2(S/I) k T_0 B_r F_n} \quad (V-8N)$$

$$R^2 = \frac{-\frac{P_j G_j G_t \lambda^2 (S/I) \left(\frac{\theta F_p}{\omega}\right)^{0.8}}{(4\pi)^2 L_p L} + \sqrt{\left(\frac{P_j G_j G_t \lambda^2 (S/I) \left(\frac{\theta F_p}{\omega}\right)^{0.8}}{(4\pi)^2 L_p L}\right)^2 + \frac{4(S/I) k T_0 B_r F_n P_t G_t^2 \lambda^2 \sigma \left(\frac{\theta F_p}{\omega}\right)^{0.8}}{(4\pi)^3 L}}}{2(S/I) k T_0 B_r F_n} \quad (V-8D)$$

These equations were coded in MATLAB and EXCEL to generate plots of the inter-relationships between these four major variables for a specific radar. A representative EXCEL program, entitled RCS-JERP, is included as an appendix. For copies of this program, please contact Dr. Robert Ball, or the author. A summary of representative values for all variables, as well as plots of JERP versus RCS for four different data combinations are presented in the Table and Figures that follow.

Table V-2: Summary of Representative Values

Parameters	A-A	Strike
P_t (kW)	5	1,500
k (J/ $^{\circ}$ K)	1.38×10^{-23}	
T_0 ($^{\circ}$ K)	290	
B_r (kHz)	7.5	1,250
F_n	7	6
L	30	6
S/N_{det}	20	10
f (GHz)	10	5
λ (m)	0.03	0.06
θ (degrees)	2.5	1.5
F_p (Hz)	1,500	1,140
ω (deg/sec)	80	120
η	0.7	NA
d (cm)	71	NA
G_t	3,529 (eq. III-15)	11,556 (eq. III-16)
B_j (kHz)	1,000	3,000
L_p	2	2

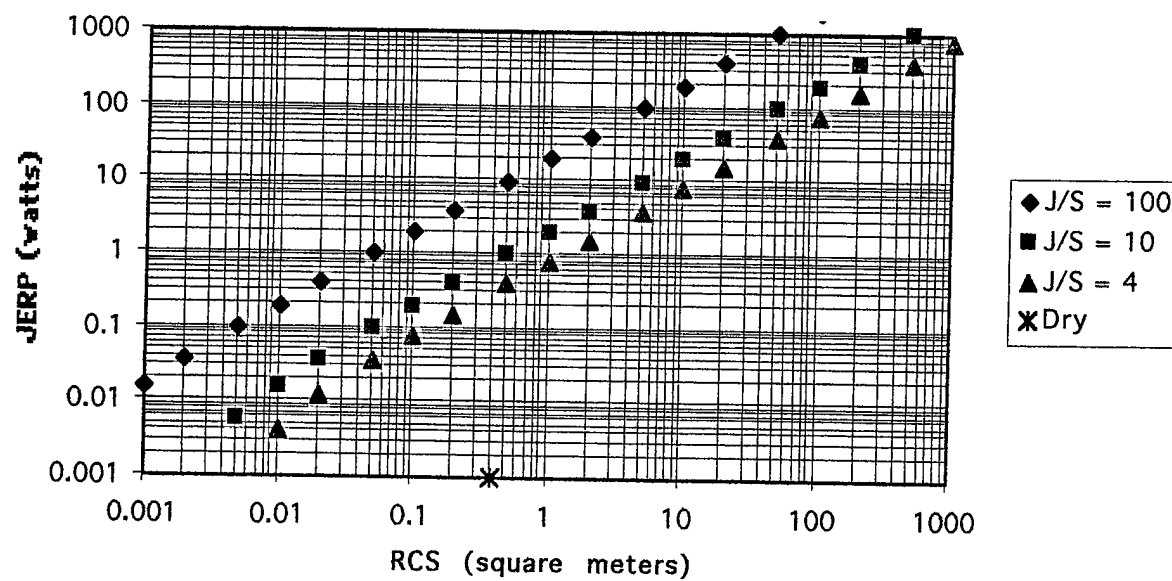


Figure V-2: Air-to-Air Scenario with Noise Jamming (Range = 35km)
 (“dry” indicates the absence of jamming.)

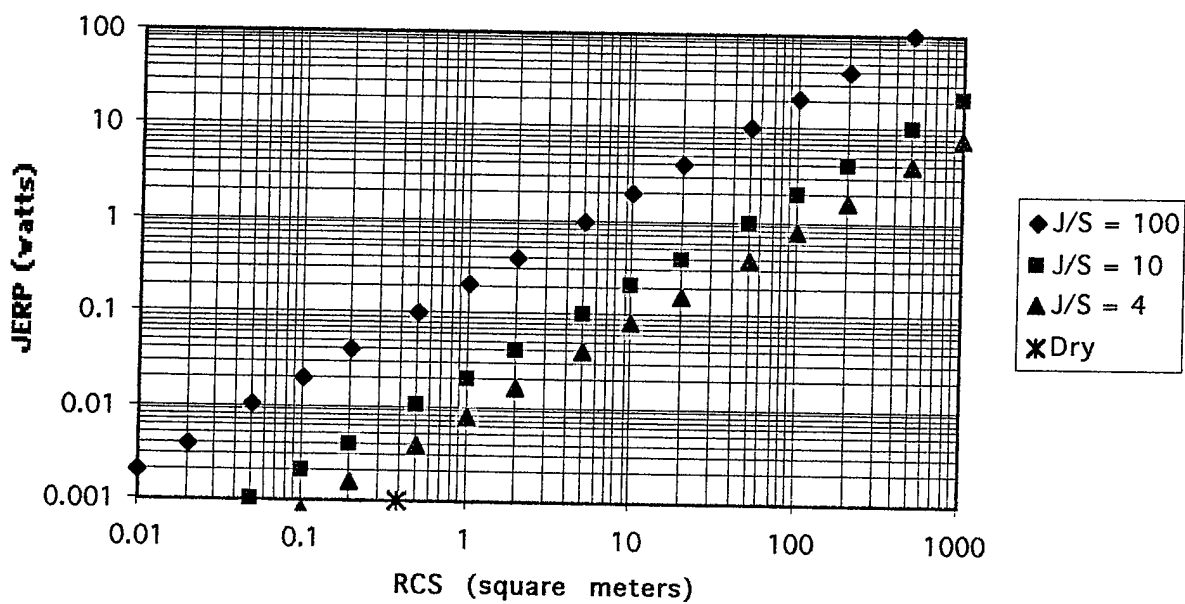


Figure V-3: Air-to-Air Scenario with Deception Jamming (Range = 35km)

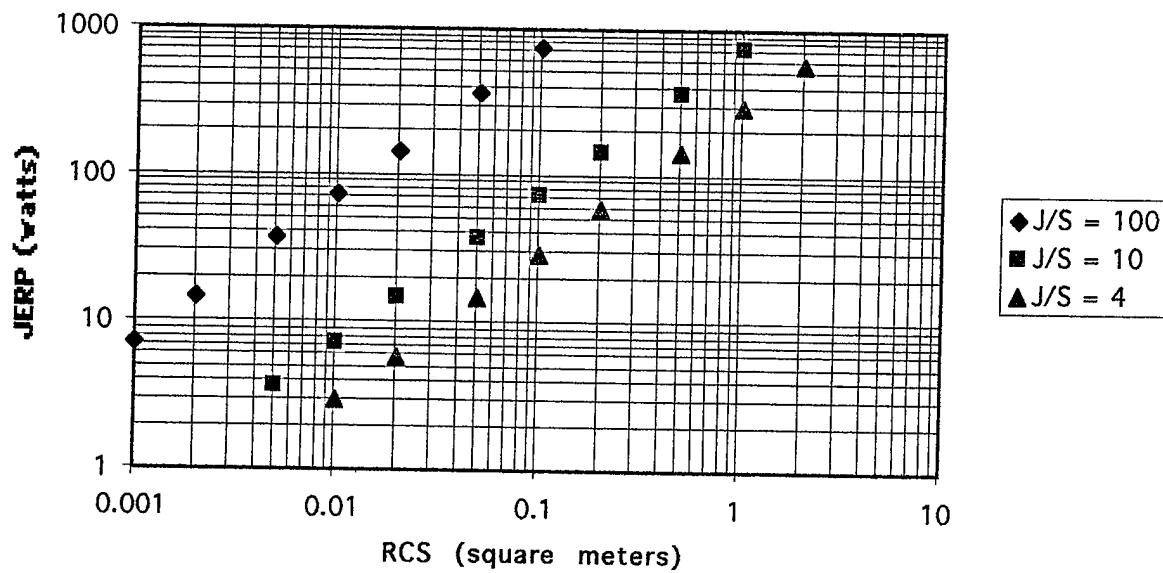


Figure V-4: Strike Scenario with Noise Jamming (Range = 11km)

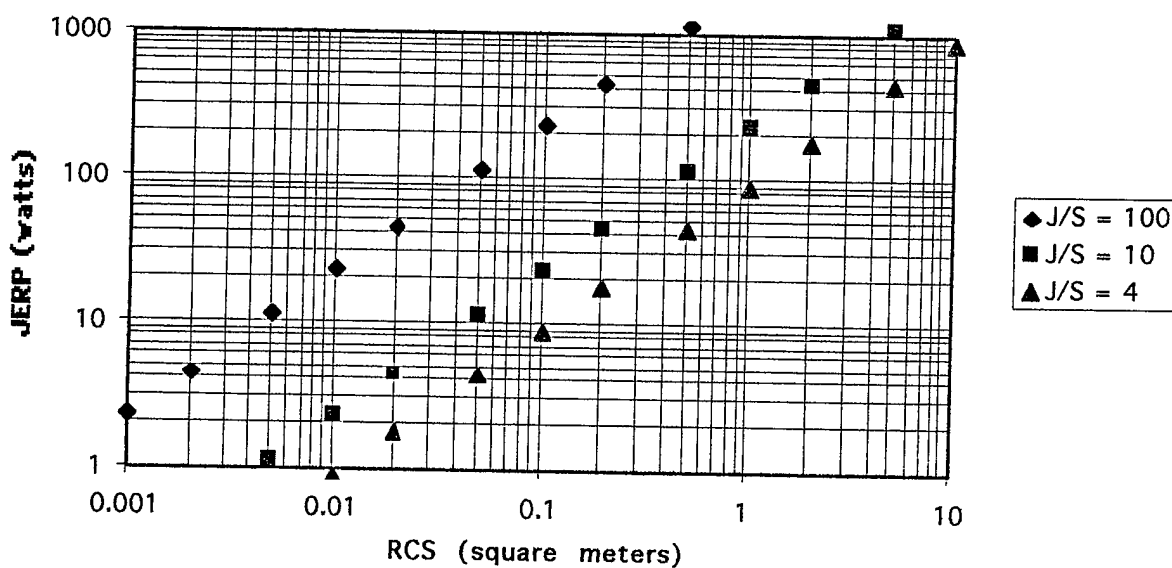


Figure V-5: Strike Scenario with Deception Jamming (Range = 11km)

Figures V-2 through V-5 provide a means for determining the combinations of RCS and JERP design specifications that meet the requirements of the mission threat analysis in terms of detection range, based upon the threat radar systems selected. It should be pointed out that the

results presented here are unique to the unclassified characterization of the two threat radar systems presented earlier. The J/S requirements will flow from a study of which techniques are determined to be effective against these threat radar systems. Once the appropriate technique is determined, the applicable figure (mission and jamming type dependent) can be entered using the required J/S associated with that technique. Presumably, the input will be an initial RCS level for which the resulting output is the JERP that will prevent targeting by the specified threat system until the required range for the desired technique. Further iteration of the RCS design specification and the associated JERP level will result in a set of specifications that will meet the requirements of the specific mission threat analysis. For EA implementations which utilize combinations of noise and deception, the worst case (in terms of JERP) should be used. It is anticipated that multiple mission threat analyses will need to be performed to find the most restrictive set of design specifications that meet the requirements of the analyses.

As an example of this methodology, assume the achievable RCS level is 1.0 square meters. The required JERP for the air-to-air scenario with deception is found in Figure V-3 as 0.008 watts for a $(J/S)_{req'd}$ of 4 and 0.2 watts for a $(J/S)_{req'd}$ of 100.

B. ADDITIONAL INFORMATION AND DATA PRESENTATION

1. Addition of Cost Data

The above plots demonstrate a nearly linear relationship when plotted in a log-log format. The curves do, however, depart linearity at low RCS and low jammer power levels as the noise power level and the jammer power level reach similar orders of magnitude. It can be safely assumed that the cost curves associated with achieving the range of RCS levels considered in this report are not linear. A similar assumption can also be made regarding the jammer power levels. Therefore, incorporation of classified cost data on the above plots will likely yield a three dimensional surface with valleys indicating areas of more "efficient", cost effective design requirements. The classification level of this report prevents exploring this option.

2. Evaluating Different Deception Techniques

The above figures are also useful in evaluating the implementation of different deception techniques. If a more effective technique is available at the expense of a much higher J/S required, it can easily be determined how much more JERP is required to implement it or how much the signature must be reduced to accommodate it, or what combinations of both will result in success. For example, if noise jamming with a required J/S of 4 is effective, but cross eye deception with a required J/S of 100 is better, one can easily determine how much additional JERP is required to support the cross eye jamming implementation and determine its feasibility.

3. Different Data Presentations

The data can be presented in many more ways to approach the design specification problem from different perspectives. Figure V-6 is a good way to explore the sensitivity of the design to S/N and J/S variations. S/I is calculated using eq. (V-1), based on the S/N for the threat radar system and the J/S of the applicable jamming technique. This value then forms the basis of a trade between the JERP and the RCS level along a constant S/I line.

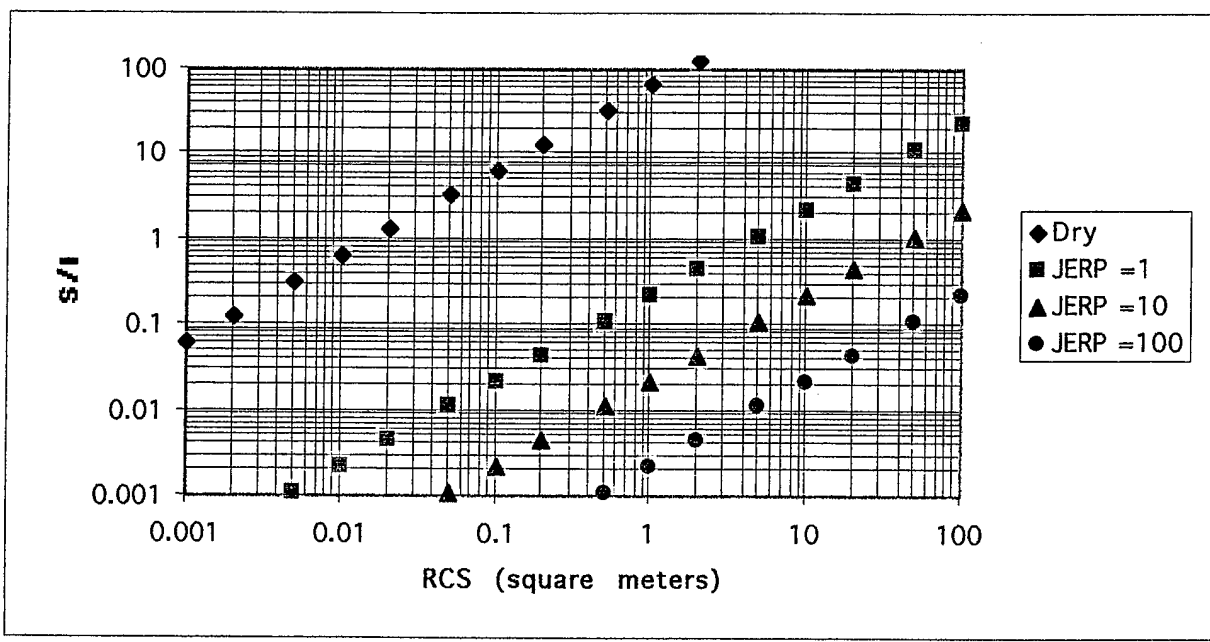


Figure V-6: Signal-to-Interference Ratio versus RCS for Slotback Radar Scenario (Range = 35km)

Another way to present the data is Figure V-7, which is a plot of detection range versus the RCS for several JERP levels at a constant S/I, using representative values from Table V-1.

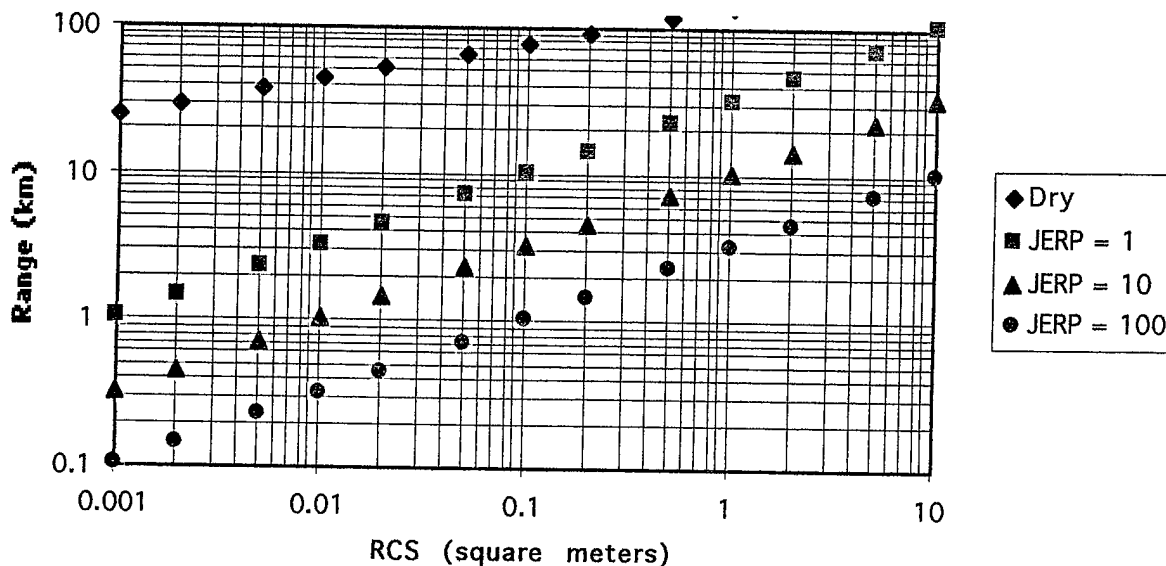


Figure V-7: Detection Range versus RCS for Slotback Radar Scenario with Noise Jamming (S/I = 0.25, from Table V-1))

Figure V-7 demonstrates the sensitivity of the detection range to very low power jamming at constant S/I. This figure is useful when the J/S of the desired technique is not subject to variation, which yields a constant S/I. A constant S/I would be the case if the EA effectiveness analysis determined that the threat radar could only be victimized by a single, unique jamming technique. However, assuming a constant S/I limits its utility in evaluating different deception techniques with varying J/S requirements as this would cause a corresponding change in S/I. The figures provide an easy means of trading range requirements against JERP and RCS, for a constant S/I, if the range requirement of the mission threat analysis is negotiable.

VI. SUMMARY, CONCLUSIONS, AND RECOMMENDATIONS

In summary, the first step in the JSF trade study between EA power and RCS level is a mission threat analysis for threats that the JSF is expected to encounter during representative missions. The mission threat analysis defines both the applicable threat radar system and the tactical advantage (in terms of detection range) which must be provided for the JSF to get the first shot off in an engagement. Once the threat system has been characterized and the pertinent radar parameters defined, potentially effective jamming techniques are considered and the required J/S ratios determined. Finally, an EXCEL spreadsheet is used to generate charts depicting acceptable combinations of JERP and RCS for comparison.

Using the methodology presented in this report, and the EXCEL spread sheet, the effects on survivability of combined RCS reduction and EA power can be evaluated. Further JSF mission threat analyses will undoubtedly be conducted involving additional threat systems. The EXCEL program used to develop the charts in Chapter V can easily be modified to incorporate data for other threat systems. The user must provide the pertinent threat radar and jammer characterization data in the upper portion of the spreadsheet. Calculations will be performed automatically in accordance with the annotated equations. Some scaling of the plots may be necessary.

It is recommended that numerous mission threat analyses be conducted on ALL threats the JSF could potentially encounter, as well as realistic estimates of future threats. These analyses should be conducted using all weapons in the U.S. arsenal that will be available to the JSF, including long range standoff weapons. From these analyses, the most stringent conditions can be determined.

In the past, analyses of susceptibility reduction features such as signature reduction and onboard EA may have focused on either RCS or JERP alone, ignoring whatever influence the other may have on the outcome. However, signature reduction and onboard EA are not mutually exclusive techniques, but should be applied synergistically. While a strong case can be made for limiting emissions on very stealthy designs, the same is not necessarily true for moderately low RCS designs. For moderately low RCS levels, detection is not always denied, but either targeting is denied (rail keeping) or the missile is deceived (very large miss distance) by the employment of onboard EA. Signature reduction and jammer capability must be evaluated for the combined effect they have on achieving mission success. Only by evaluating all capabilities in concert with one another can a cost efficient design solution be reached.

It should also be clear that this type of trade-off analysis MUST be performed in the early design stages of the aircraft. The inclusion of cost data in the design optimization will help determine that combination of RCS level and JERP that meets the tactical requirements at the minimum cost. The end result will be a survivable, cost effective aircraft!

APPENDIX

RCS-JERP

Radar			Jammer		
Power	5000	watts	B_J	1000000	Hz
Gain	3500		$J/S_{req'd}$	4	
λ	0.03	meters	p	2	
L	30				
k	1.4E-23	Ws/K			
T_o	290	K			
Br	7500	Hz			
F_N	7				
$S/N_{req'd}$	20				
ω	80	deg/sec			
θ	2.5	deg			
PRF	1500	Hz			
			JERP (W)		J
			1	5.5E-14	
			5	2.7E-13	
			10	5.5E-13	
			50	2.7E-12	
			100	5.5E-12	
			200	1.1E-11	

S/I vs RCS

(eq V-4)

$$I = 21.71$$

$$\text{Noise Power} = 2.1E-16$$

$$R_{max} (\text{km}) = 37$$

	RCS	10	5	2	1	0.5	0.2	0.1
S/N	Dry	23.5	11.8	4.7	2.4	1.2	0.5	0.2
S/I (1)	JERP = 1	1.956	0.978	0.391	0.196	0.098	0.039	0.020
S/I (10)	JERP = 10	0.196	0.098	0.039	0.020	0.010	0.004	0.002
S/I(100)	JERP = 100	0.020	0.010	0.004	0.002	0.001	0.000	0.000
S at Radar		4.9E-15	2.5E-15	9.9E-16	4.9E-16	2.5E-16	9.9E-17	4.9E-17

JERP vs RCS

(eq V-7N)

$$S/I = 0.01 \quad 0.01$$

$$S/I = 0.10 \quad 0.10$$

$$S/I = 0.25 \quad 0.25$$

	RCS	10	5	2	1	0.5	0.2	0.1
JERP	S/I = 0.01	196.344	98.1699	39.2656	19.6309	9.81353	3.9231	1.95963
	S/I = 0.10	19.6309	9.81353	3.9231	1.95963	0.97789	0.38885	0.1925
	S/I = 0.25	7.85005	3.9231	1.56693	0.78154	0.38885	0.15323	0.07469

Range vs RCS		J(0)	0		
(eq V-9N)		J(1)	7.5E-05	S/I =	0.25
		J(100)	0.00748		
		J(200)	0.01496		

	RCS	10	5	2	1	0.5	0.2	0.1
R (0)	Dry	248.739	209.164	166.342	139.876	117.621	93.5408	78.6581
R (1)	JERP = 1	102.203	72.7817	46.2338	32.741	23.1687	14.6598	10.3676
R (100)	JERP = 100	10.3692	7.33211	4.63724	3.27902	2.31862	1.46642	1.03692
R (200)	JERP = 200	7.33211	5.18459	3.27902	2.31862	1.63951	1.03692	0.73321
R ² (0)		6.2E+10	4.4E+10	2.8E+10	2E+10	1.4E+10	8.7E+09	6.2E+09
R ² (1)		1E+10	5.3E+09	2.1E+09	1.1E+09	5.4E+08	2.1E+08	1.1E+08
R ² (100)		1.1E+08	5.4E+07	2.2E+07	1.1E+07	5375992	2150397	1075199
R ² (200)		5.4E+07	2.7E+07	1.1E+07	5375992	2687996	1075199	537599
S = S(R)		9259.72	4629.86	1851.94	925.972	462.986	185.194	92.5972

LIST OF REFERENCES

Ball, Robert E., "The Fundamentals of Aircraft Combat Survivability Analysis and Design," AIAA Education Series, AIAA, New York, New York, 1985.

Ball, Robert E., "The Fundamentals of Aircraft Combat Survivability Analysis and Design," 2nd Edition (Rough Draft) , 1997.

Kopp, Carlo, "A New Paradigm for the F-111," Air Power Studies Centre, 1996.

Levien, Frederick, "EC4680 Class Notes," Naval Postgraduate School, Monterey, California, Spring Quarter, 1997.

Schleher, Curtis D., "Introduction to Electronic Warfare," Artech House, Norwood, Massachusetts, 1986.

Skolnick, Merrill I., "Introduction to Radar Systems," McGraw-Hill, Inc., New York, New York, 1980.

Stimson, George W., "Introduction to Airborne Radar," Hughes Aircraft Company, El Segundo, California 1983.

Stutzman, Warren L. and Thiele, Gary A., "Antenna Theory and Design," John Wiley and Sons, Inc., New York, New York, 1981.

"Aircraft Nonnuclear Survivability Terms MIL-STD-2089," Department of Defense, Washington, DC, 1981.

"Jane's All the World's Aircraft," Jane's Information Group, Surrey, UK, 1996.

SELECTED BIBLIOGRAPHY

Adamy, Dave, "EW 101 Tutorial," *Journal of Electronic Defense*, July 1995 - April 1997.

Chrzanowski, Edward J., "Active Radar Electronic Countermeasures," Artech House, Norwood, Massachusetts, 1990.

Golden, August Jr., "Radar Electronic Warfare," AIAA Education Series, AIAA, New York, New York, 1987.

Hoisington, D.B., "Electronic Warfare," Naval Postgraduate School, Monterey, California.

Knott, Eugene F., Schaeffer, John F., and Tuley, Michael T., "Radar Cross Section," Artech House, Norwood, Massachusetts, 1993.

Kopp, Carlo, "Report: RAAF F-18s Would Be Outgunned in Air-to-Air Combat," *Journal of Electronic Defense*, p. 55, May 1997.

Payne, Keith B. and Kohout, John J. III, "The B-2 Bomber, Air Power for the 21st Century," University Press of America, Inc., Lanham, Maryland, 1995.

Van Brunt, Leroy B., "Applied ECM volume 1," EW Engineering, Inc., Dunn Loring, Virginia, 1978.

"Jane's Avionics," Jane's Information Group, Surrey, UK, 1996.

"Jane's Radar and Electronic Warfare Systems," Jane's Information Group, Surrey, UK, 1996.

INITIAL DISTRIBUTION LIST

	No. Copies
1. Defense Technical Information Center 8725 John J. Kingman Road, Ste 0944 Ft. Belvoir, VA 22060-6218	2
2. Dudley Knox Library Naval Postgraduate School 411 Dyer Rd. Monterey, CA 93943-5101	2
3. Dr. Robert Ball, Code AA/Bp Department of Aeronautics and Astronautics Naval Postgraduate School Monterey, CA 93943-5000	1
4. Capt. James Powell, USN, Code IW/PI Department of Information Warfare Naval Postgraduate School Monterey, CA 93943-5000	1
5. Dr. Fred Levien, Code IW/Lv Department of Information Warfare Naval Postgraduate School Monterey, CA 93943-5000	1
6. Dr. Rick Howard, Code AA/Ho Department of Aeronautics and Astronautics Naval Postgraduate School Monterey, CA 93943-5000	1
7. LCDR Brian Flachsbart 347 Ridge Meadow Dr. Chesterfield, MO 63017	1
8. LCDR Mike Overs 137 Moreell Monterey, CA 93940	1
9. Dr. Barry Flachsbart 347 Ridge Meadow Dr. Chesterfield, MO 63017	1
10. Program Executive Officer-Tactical Aircraft (PMA-272) Attn: Capt Doug Henry, USN 1421 Jefferson Davis Highway Arlington, VA 22243	2

11.	Joint Strike Fighter Program Office Attn: Maj Laurie Rouillard, USAF 1745 Jefferson Davis Hwy Suite 307 Arlington, VA 22202	1
12.	Joint Strike Fighter Program Office Attn: CDR Russell Scott, USN 1745 Jefferson Davis Hwy Suite 307 Arlington, VA 22202	1
13.	COL J. G. Upton, USMC 2000 Navy Pentagon Washington, D.C. 20350-2000 Code N880M Rm 4E384	2
14.	Commander, Naval Air Warfare Center, Weapons Division Code 418200D 1 Administration Circle China Lake, CA 93555 Attn: Roy Randolph	1
15.	Commander, Naval Air Warfare Center, Weapons Division Code 418100D 1 Administration Circle China Lake, CA 93555 Attn: Bryan Lail	1
16.	Mr. Paul Wiedenhaefer 1600 Spring Hill Rd. Suite 400 Vienna, VA 22182	1
17.	Mr. John Donis Institute for Defense Analysis 1801 N. Beauregard St. Alexandria, VA 2231-1772	1
18.	Mr. Dave Adamy 1587 Vireo Avenue Sunnyvale, CA 94087	1
19.	Lt Col (P) Dave Bujold, USAF P.O. Box 50615 Henderson, NV 89016	1
20.	Mr. Pete Sharp P.O. Box 50615 Henderson, NV 89016	1
21.	Department of Aeronautics and Astronautics Naval Postgraduate School Monterey, CA 93943-5000	1